

Scalable Multicopter UAV Trajectory Planning using Mixed-Integer Linear Programming

Jorik De Waen

Thesis voorgedragen tot het behalen
van de graad van Master of Science
in de ingenieurswetenschappen:
computerwetenschappen, hoofdoptie
Artificiële intelligentie

Promotor:

Prof. dr. T. Holvoet

Assessoren:

Dr. M. Cruz Torres

Dr. B. Bogaerts

Begeleiders:

H. T. Dinh

Dr. M. Cruz Torres

© Copyright KU Leuven

Without written permission of the thesis supervisor and the author it is forbidden to reproduce or adapt in any form or by any means any part of this publication. Requests for obtaining the right to reproduce or utilize parts of this publication should be addressed to the Departement Computerwetenschappen, Celestijnenlaan 200A bus 2402, B-3001 Heverlee, +32-16-327700 or by email info@cs.kuleuven.be.

A written permission of the thesis supervisor is also required to use the methods, products, schematics and programmes described in this work for industrial or commercial use, and for submitting this publication in scientific contests.

Zonder voorafgaande schriftelijke toestemming van zowel de promotor als de auteur is overnemen, kopiëren, gebruiken of realiseren van deze uitgave of gedeelten ervan verboden. Voor aanvragen tot of informatie i.v.m. het overnemen en/of gebruik en/of realisatie van gedeelten uit deze publicatie, wend u tot het Departement Computerwetenschappen, Celestijnenlaan 200A bus 2402, B-3001 Heverlee, +32-16-327700 of via e-mail info@cs.kuleuven.be.

Voorafgaande schriftelijke toestemming van de promotor is eveneens vereist voor het aanwenden van de in deze masterproef beschreven (originele) methoden, producten, schakelingen en programma's voor industrieel of commercieel nut en voor de inzending van deze publicatie ter deelname aan wetenschappelijke prijzen of wedstrijden.

Preface

TODO: preface

Jorik De Waen

Contents

Preface	i
Abstract	iv
Samenvatting	v
List of Figures	vi
List of Tables	x
1 Introduction	1
1.1 Motivation	1
1.2 Contribution	2
1.3 Structure of the Thesis	2
1.4 Literature Review	3
1.5 goals	4
1.6 Assumptions	4
1.7 TODO: explain title	4
2 Modeling Trajectory Planning as a MILP problem	5
2.1 Introduction	5
2.2 Overview of MILP	5
2.3 Time and UAV state	7
2.4 Objective function	7
2.5 Vehicle state limits	9
2.6 Obstacle avoidance	10
3 Segmentation of the MILP problem	15
3.1 Algorithm approach	15
3.2 Finding the initial path	17
3.3 Detecting turn events	21
3.4 Generating path segments	22
3.5 Generating the active region for each segment	26
4 Extensions	29
4.1 Solver-specific improvements	29
4.2 Corner cutting	30
4.3 Stability Improvements	32

4.4	Overlapping segment transitions	35
4.5	Graphical Visualization Tool	36
5	Experiments and Results	43
5.1	Scenarios	43
5.2	General Performance	51
5.3	Agility of the UAV	54
5.4	Stability	59
5.5	Cornercutting	61
5.6	Linear approximation	62
5.7	Time step size	63
5.8	Max Time	64
5.9	Approach Margin	65
5.10	Genetic Algorithm Parameters	66
6	Discussion	67
6.1	Research question result	67
6.2	Factors	68
6.3	Critical Review	69
7	Degree of Non-convexity	71
7.1	Scenarios	71
7.2	Results	71
7.3	Discussion	73
8	Conclusions	75
8.1	Future work	75
8.2	actual contribution	76
8.3	goals reached?	76
8.4	challenges	76
	Bibliography	77

Abstract

TODO: english abstract

Samenvatting

TODO: dutch abstract

List of Figures

2.1	A visualization of the linear approximation for the 2-norm	9
2.2	A visual representation of how obstacle avoidance works. The top image shows the vehicle's current position as the filled circle, with its path in previous time steps as hollow circles. The color of the edges of the obstacle represent whether or not the vehicle is in the safe zone for that edge. An edge is yellow if the vehicle is in the safe zone, and red otherwise. The middle image shows the safe zone defined by a yellow edge in yellow. Note how the vehicle is on one side of the black line and the obstacle is entirely on the other side. The bottom image shows an edge for which the vehicle is not in the safe zone (represented in red this time). As long as the vehicle is in the safe zone of at least one edge, it cannot collide with the obstacle.	11
2.4	A geometric proof for the vehicle offset formula in Equation 2.29. Measures are marked in blue. P is the center of mass of the UAV. d is the line defined by edge i of an obstacle. The obstacle is the orange region. We wish to translate d vertically to d' such that when the UAV's center of mass P touches d' , the circle with radius r (representing the UAV's shape, colored in grey) touches d in Q . If d' is used for the constraint instead of d , the UAV cannot collide with the obstacle. The difference between the intercepts of d and d' is $v_i = PM $. The slope of d' is a_i , so if XY is horizontal and $ XY = 1$, then $ MY = a_i$. Corner M is the same in both triangle PQM and XYM , as marked in red. Corner Q and Y are both right angles. This means PQM and XYM are similar triangles. As a result: if $ PQ = r$, then $ QM = a_i r$. Using Pythagoras' theorem: $v_i = \sqrt{r^2 + a_i^2 r^2} = r\sqrt{1 + a_i^2}$	13
3.1	An example of how a grid is used to build the graph for the path finding algorithm. Each point is a node on the graph. If two points are connected by a line, their nodes in the graph also are connected by an edge. Diagonal edges are not shown here for clarity.	17
3.2	The red line shows a typical A* path, compared to the path found by Theta*. The gray rectangle is an obstacle.	18

3.3	The left image shows the results after the Theta* algorithm has executed. The blue shapes are obstacles, while the gray line is the Theta* path. The right image shows the results after the path is segmented. Extra nodes have been added to the Theta* path, as marked by the green circles. These circles depict the transitions between segments.	23
3.4	The left image shows the result after the genetic algorithm has executed. The obstacles in red have been selected to be modeled in the MILP problem. The dark grey shape is the convex allowed region generated by the genetic algorithm. Note how it does not overlap with any of the blue obstacles. The right image shows the final result. The trail of circles show the path of the vehicle up to the current time step, which is represented by the filled circles. The red and yellow colors depict the same information as in figure 2.2	24
3.5	genetic convexity example	27
4.1	An example of corner cutting	30
4.2	These images are three consecutive time steps which demonstrate how the corner cutting prevention works. In 4.2a, the UAV is in the safe region of the left edge (which is indicated by the yellow color). In 4.2c, the UAV is in the safe region for the right edge, but not the left edge. To ensure that the UAV does not cut the corner, the UAV must enter the safe region of the right edge before it exits the safe region of the left edge. The intersection between those two safe regions is the inverted yellow triangle in 4.2b. If the UAV spends at least one time step in that yellow, it cannot cut the corner.	31
4.3	4.3a shows the UAV right before a reaching its goal. The blue circle shows the position of the UAV at the segment transition. The goal position is the green dot, while the square around it show the tolerance region where the goal is considered to be reached. Note how the segment transition happens earlier because of the tolerance region. 4.3b shows the same, only this time a (blue) finish line is added. This time, the UAV needs to cross the finish line so it so the segment transition is roughly as far along the path as planned.	32
4.4	A visual demonstration of when a maximum goal velocity is used. Points B and D are individual turn events. The segment for event B starts at A, with $ AB $ being the desired expansion distance for the segment. However, because D is so close to B, the end of the segment C cannot be placed at the desired expansion distance from B. Instead, C is placed in the middle between B and D, such that $ BC = CD $. The first segment solves the trajectory from A to C past turn event B, the second segment starts as C, past D and onwards. The goal is to ensure that the UAV can still safely stop at D when it starts the second segment at C. This is done by limiting the maximum velocity of the UAV when it reaches the goal C in the first segment.	33

4.5	An example of how transition between segments can fail. In 4.5a, shows the UAV right before the segment transition which happens at the blue circle. 4.5b shows the orange initial safe region and dark grey expanded safe region of the next segment, after the transition. The next segment fails to solve because the UAV cannot come to a stop within the safe region. The position of the UAV shows where the UAV came to a stop in the previous segment (the safe region of which is the grey region in 4.5a).	34
4.6	4.6a shows the initial safe region without the extra stop points in orange. 4.6b shows the initial safe region with the extra stop points. The position marked with "1" is the stop point for the initial velocity, while the position marked with "2" is the stop point for the trajectory after the goal has been reached. 4.6c shows how the stop point ensured that the UAV could stop. The UAV leaves the initial safe region because it already has started to turn, however the stop point clearly provided enough space.	34
4.7	4.7a and 4.7 show the trajectory respectively without and with the maximum goal velocity enabled. In 4.7a, the UAV overshoots the corner which results in a slower trajectory.	35
4.8	4.8a shows the optimal approach to the goal of the previous segment. However, as seen in 4.8b, this is a very bad start state for the next segment. By starting the next segment 5 time steps earlier in 4.8c, this bad approach for can be partially mitigated.	36
4.9	An overview of the visualization tool that shows the results of the algorithm.	37
4.10	Visualization of the obstacles, initial path, turn events and segment goals	39
4.11	Visualization of the safe region, obstacle edge constrain state and the segment transitions.	40
4.12	Visualization of the initial safe region and the segment goal conditions .	41
5.1	The parameters used for testing	44
5.2	The synthetic scenarios	46
5.3	A zoomed-in view of the first small the San Francisco scenario	47
5.4	The San Francisco scenarios	48
5.5	A zoomed-in view of the first small the Leuven scenario	49
5.6	The Leuven scenarios	50
5.7	52
5.8	56
5.9	57
5.10	58
5.11	stability data	59
5.12	A case where the transition between segments fails	60
5.13	60
5.14	The error bars show the 95% confidence interval.	61
5.15	linear approx data	62
5.16	time step data	63

5.17	maxtime data	64
5.18	approach data	65
7.1	Three different testing scenarios, each with the same amount of obstacles. In each scenario, the UAV needs nearly the same amount of time steps to reach its goal. The only difference is the layout of the obstacles.	72
7.2	Performance of the MILP problem.	73
7.3	74

List of Tables

5.1	The UAV properties for the synthetic scenarios	45
5.2	The UAV properties for the San Francisco scenarios	47
5.3	The UAV properties for the Leuven scenarios	49
5.4	Some information about the scenarios tested.	51
5.5	A breakdown of the execution time for each scenario, as well as the score of the trajectory.	51
5.6	A breakdown of the execution time per segment	52
5.7	The different maximum velocity and acceleration values for the vehicle for the Up/Down scenario.	54
5.8	The different maximum velocity and acceleration values for the vehicle for the San Francisco and Leuven scenarios.	54
5.9	Up/Down	55
5.10	San Francisco	55
5.11	Leuven	55

Introduction

As a consequence of ever-increasing automation in our daily lives, more and more machines have to interact with and unpredictable environment and other actors within that environment. One of the sectors that seems like it will change dramatically in the near future is the transportation industry. Autonomous cars are actually starting to appear on public roads, autonomous truck convoys are being tested and large retail distributors like Amazon are investing heavily into delivering order by drones instead of courier. While these developments look promising, there are still many challenges that prevent these systems from being widely deployed.

One such challenge, which is especially important for areal vehicles, is path planning. Even though most modern quadcopters are capable of flying by themselves, they are unable to generate a flight path that will get them to their destination reliably. Classic graph-based shortest path algorithms like Dijkstra's algorithm its many variants fail to take momentum and other factors into account. Mixed Integer Linear Programming (MILP) is one approach that shows promising results, however it is currently severely limited by computational complexity.

1.1 Motivation

One of the main advantages of using a constraint optimization approach like MILP is that they are extremely extendable by design. A system based on this can be deployed in many different scenarios with different goals and constraints without the need for significant changes to the algorithms that drive it. The solvers that construct the final path are general solvers which take constraints and a target function as input. This input can be generated by end users in the field to match their specific requirements, making the software controlling the drones as flexible as the hardware.

That flexibility is also the main limitation of using constraint optimization. The solvers are general purpose, which make them very slow compared to more direct approaches. They need to be carefully guided solve all but the most basic scenarios in a reasonable amount of time. While there have been some good results on small scales, I could not find any attempts at planning paths on the order of kilometers or more. Practical use cases involving drones often involve several minutes of flight and can cover several kilometers, so a path planner must be able to work at such a scale. This is the main goal of this thesis: To demonstrate how a MILP approach can be

scaled to scenarios with a much larger scope, while preserving the advantages that make it interesting.

1.2 Contribution

The goal for this thesis is to build an algorithm that uses Mixed-Integer Linear Programming for UAV trajectory planning. The algorithm must be scalable so it can handle long trajectories through large environments with many obstacles.

Through my literature study I have not been able to find previous work which has focused entirely on the scalability aspect of MILP trajectory planning. This thesis presents an approach which can scale to large and complex environments. While there is plenty of room for improvement, this new approach is the main contribution of this thesis.

The experiments performed to test the algorithm also point to some ways the approach can be adapted to improve the performance and quality of the generated trajectory. Due to time constraints I was unable to test these adaptations, but they provide interesting leads for further research.

Furthermore, towards the end of the project I came up with an hypothesis of what makes the trajectory planning problem scale so poorly. This hypothesis would also explain why my new approach is actually effective. This hypothesis came very late into the project, and has barely been explored at all. Further research to test this hypothesis could lead to a better understanding of the problem.

1.3 Structure of the Thesis

Section ?? summarizes the previous work that has been done in the field. The previous work in the field shows a common design to modeling the path planning problem as a MILP problem. This design forms the core of the approach in this thesis as well. Section ?? shows the implementation of this common design and explores the critical limitations to this approach.

Section 3 proposes a solution to these limitation. By finding a rough initial path, the planning problem can be split into smaller segments. Solving these segments on their own is significantly easier and can still enforce all the constraints. This approach is much faster than previous techniques, but at the cost of no longer finding the global optimum.

During the development of this algorithm, finding and solving bugs and other unwanted behavior proved to be a significant challenge. A visualization tool was developed to make it easier to see how the algorithm operates. Section 4.5 goes into detail of how nearly every variable in the MILP problem was visualized and how this information can be interpreted.

To demonstrate the flexibility of the approach, section ?? showcases some possible extensions that can be added with relative ease. Some of these have been fully implemented to look at the impact on the solution. This section should demonstrate that the path planner discussed in this thesis is a modular strategy built out of

several different algorithms. The specific algorithms discussed are just one way of doing things, and can be easily swapped out for other, more advanced, algorithms.

Section ?? analyzes the performance of the path planner in several different scenarios. It also looks at how the extensions which have been implemented affect the both the performance and quality of the planner. Finally, section ?? summarizes the main observations in this thesis and concludes whether or not the goals have been realized.

1.4 Literature Review

Schouwenaars et al. [12] were the first to demonstrate that MILP could be applied to path planning problems. They used discrete time steps to model time with a vehicle moving through 2D space, just like the approach we present in this paper. The basic formulations of constraints we present in this paper are the same as in the work of Schouwenaars et al. To limit the computation complexity, they also presented a receding horizon technique so the problem can be solved in multiple steps. However, this technique was essentially blind and could easily get stuck behind obstacles. Bellingham[1] recognized that issue and proposed a method to prevent the path from get stuck behind obstacles, even when using a receding horizon.

Flores[7] and Deits et al[5] do not use discretized time, but model continuous curves instead. This not possible using linear functions alone. They use Mixed Integer Programming (MIP) with functions of a higher order to achieve this. The work by Deits et al. is especially relevant to this paper, since they also use convex regions to limit (or in their work: completely eliminate) the need to model obstacles directly.

Several papers [6, 8, 3, 10] show how the output from algorithms like these can be translated to control input for an actual physical vehicle. This demonstrates that, when they properly model a vehicle, these path planners need minimal post-processing to control a vehicle. Of course that does assume these planners can run in real time to deal with errors that inevitably will grow over time. Culligan [4] provides an approach built with real time operation in mind. Their approach only finds a suitable path for the next few seconds of flight and updates that path constantly. TODO: explain better

More work has been done on modeling specific kinds of constraints or goal functions. For instance, Chaudhry et al. [2] formulated an approach to minimize radar visibility for drones in hostile airspace. However, none of these have really attempted to make navigating through a complex environment like a city feasible. The approach by Deits et al. [5] could work, but did not really explore the effects of longer paths on their algorithm.

TODO:PRM and RERT

1. INTRODUCTION

1.5 goals

1.6 Assumptions

1.7 TODO: explain title

Modeling Trajectory Planning as a MILP problem

2.1 Introduction

This section covers how a trajectory planning problem can be represented using Mixed Integer Linear Programming. This is a relatively simple model based on the work by Bellingham [1]. This model by itself is sufficient to solve the trajectory planning problem, but its poor scalability prevents it from being used on any but the most basic scenarios.

Section 2.2 starts out with a basic overview of what MILP is, highlighting its strengths and weaknesses. Section 2.3 to 2.6 describe how I modeled the trajectory planning problem.

2.2 Overview of MILP

2.2.1 Mathematical Programming

Mixed integer linear programming is an extension of linear programming, which is in turn a form of mathematical programming. In mathematical programming, problems are represented as models. Each model has some amount of unknown decision variables. Models are solved by assigning values to those decision variables. To accurately represent most problems, a model also needs constraints. Constraints are mathematical equations which determine the allowed values for each decision variable. When all decision variables have values which are allowed by the constraint, the constraint is called "satisfied".

In mathematical programming, solvers are used to assign values to variables in a model. The goal of a solver is to assign those values while ensuring that all constraints are satisfied. For many problems (and their corresponding models), this is extremely challenging. Only one solution may exist among a near infinite amount of options. In many cases, the goal is not to find just any solution to the problem, but to find the best possible solution. The quality of a solution is determined by an objective function. The solver aims to find the solution with the highest (or lowest) score based on the objective function, while also keeping all constraints satisfied. When

an objective function is present, these problems are called optimization problems.

2.2.2 Mixed Integer Linear Programming

Solving these general mathematical models turns out to be extremely hard (TODO: cite). By limiting how a problem can be expressed in a model, it becomes much easier to build a solver which can efficiently solve those models. This is where Linear Programming (LP) comes in. In LP, all constraints must be linear equations. The objective function must also be a linear function. The decision variables must be real values.

Under those limitations, LP problems can be solved quickly and reliably (TODO: cite). However, the kinds of problems that can be modeled using LP is very limited. It is impossible to model "OR" (\vee) relations, conditionals (\rightarrow) and many other logical relations. It also prevents the use of common mathematical functions like the absolute value, among others (TODO: cite?).

Many of those limitations can be resolved by allowing some (or all) of the decision variables to be integers [11]. While variables could take on integer values in LP, there is no way to limit the domain of a variable so it can only take on integer values. This extension is called Mixed-Integer Linear Programming (MILP). LP alone is not sufficient to model a trajectory planning problem, so MILP is required.

The addition of integer variables makes MILP much harder to solve than LP. MILP belongs to a class of problems called "NP-Complete". Problems which belong to this class tend to quickly become too difficult to solve in an acceptable amount of time when the size of the problem is increased. For MILP, the worst case difficulty grows exponentially with the amount of integer variables.

2.2.3 Arguments for MILP

The poor worst case performance is the main disadvantage of MILP, but it also has advantages over other approaches.

The main advantage is flexibility. Mathematical Programming is a form of declarative programming. In imperative programming, the programmer needs to describe step-by-step how the algorithm should solve a specific kind of problem. Even a small change to the problem may cause large changes to how the algorithm works.

In declarative programming, the programmer does not tell the computer exactly how to solve the problem. A general solver does the heavy lifting and finds the solution. This means that when the problem changes slightly, the model only needs to be updated to reflect that small change.

Performance could actually be an advantage. Planning a good trajectory is not a trivial problem, so performance is likely to be a concern for any competing algorithm. MILP solvers have been used in other industries for decades, so a lot of work has gone in to making those solvers fast and memory-efficient. The performance of MILP approach could be comparable to, or even exceed, the performance of other algorithms.

2.3 Time and UAV state

The trajectory planning problem can be represented using discrete time steps. The state of the UAV (position, velocity, etc.) is defined at each time step. Time steps are spaced out regularly, with Δt between them. The progression of time is modeled by Equation 2.1 and 2.2. $time_n$ represents the amount of time that has passed at a given time step n . Equation 2.1 initializes the time at the first time step to be zero. Equation 2.2 progresses time by Δt at each time step. In total, there are N time steps.

$$time_0 = 0 \quad (2.1)$$

$$time_{n+1} = time_n + \Delta t, \quad 0 \leq n < N - 1 \quad (2.2)$$

The position of the UAV at time step n is represented by p_n . Equation 2.3 initializes the position in the first time step to the starting position p_{start} . Equation 2.4 updates the position of the UAV in the next time step, based on the velocity v_n in the current time step and time step size Δt . When a variable is in **bold**, it represents a vector instead of a scalar value.

$$\mathbf{p}_0 = \mathbf{p}_{start} \quad (2.3)$$

$$\mathbf{p}_{n+1} = \mathbf{p}_n + \Delta t * \mathbf{v}_n \quad 0 \leq n < N - 1 \quad (2.4)$$

The velocity of the UAV is modeled the same way as the position. Equation 2.5 initialized the velocity in the first time step, and Equation 2.6 updates it at each time step based on the acceleration \mathbf{a}_i . Other derivatives can be modeled like this as well.

$$\mathbf{v}_0 = \mathbf{v}_{start} \quad (2.5)$$

$$\mathbf{v}_{n+1} = \mathbf{v}_n + \Delta t * \mathbf{a}_n \quad 0 \leq n < N - 1 \quad (2.6)$$

2.4 Objective function

The objective for the solver is to minimize the amount of time steps before the UAV reaches the goal position. Equation 2.7 describes this. $done_n$ is a boolean variable which is *true* when the UAV has reached the goal on or before time step n . A boolean variable is an integer variable which can only be 0 (false) or 1 (true).

$$\text{minimize} \quad - \sum_{n=0}^{n < N} done_n \quad (2.7)$$

The value of $done_{n+1}$ at time step $n + 1$ is true if either $done_n$ is true, or a state transition $cdone_{n+1}$ occurs. $cdone_{n+1}$ is true whenever all conditions for reaching the goal have been satisfied. This is expressed in Equation 2.8.

$$done_{n+1} = done_n \vee cdone_{n+1}, \quad 0 \leq n < N - 1 \quad (2.8)$$

This formulation is nearly correct, but fails to address two important assumptions. The first assumption is that the UAV has not reached its goal at the start of the trajectory. $done_0$ is not constrained by Equation ??, so a valid (and optimal) solution would be setting $done_0$ to *true*. Equation 2.9 resolves this issue by forcing $done_0$ to be false.

$$done_0 = 0 \quad (2.9)$$

Similarly, no constraints actually force the UAV to reach its goal. The value of the objective function would be poor, but the solution would be valid. Equation 2.10 forces $done_{N-1}$ to be true at the last time step. In combination with Equation 2.8 and 2.9, this ensures that the UAV must reach its goal eventually for the solution to be valid.

$$done_{N-1} = 1 \quad (2.10)$$

To model the state transition, represented by $cdone_n$, Lamport's [9] state transition axiom method was used. This method separates the value of the state ($done_n$) from the requirements for transition ($cdone_n$). Equation 2.8 is the first part: It expresses that the state changes when a transition event occurs. It is not concerned with what leads to that state transition.

The second part is Equation 2.11: It describes the requirements for a state transition to occur. In this case, the UAV must be at its goal position (represented by $cdone_{p,n}$) and not be done already at time step n .

$$cdone_n = cdone_{p,n} \wedge \neg done_n \quad 0 \leq n < N \quad (2.11)$$

The equations discussed so far are all in a general form which apply to a UAV moving through a world with an arbitrary amount of spatial dimensions. For this thesis, the assumption is that the UAV moves through a 2D world. Starting from Equation 2.12, some equations only apply to 2D worlds for simplicity.

Equation 2.12 defined when the UAV is considered to be at the goal position. x_n and y_n are the UAV's 2D coordinates at time step n , while x_{goal} and y_{goal} are the coordinates of the goal position. The UAV has reached the goal if each coordinate is at most ϵ_p away from the goal's matching coordinate

$$cdone_{p,n} = |x_n - x_{goal}| < \epsilon_p \wedge |y_n - y_{goal}| < \epsilon_p, \quad 0 \leq n < N \quad (2.12)$$

Adding additional requirements for the state transition is easy. As an example, we may wish to ensure that the UAV stops at its goal. Equation 2.11 can be extended with a $cdone_{v,n}$ requirement as shown in 2.13. $cdone_{v,n}$ is defined by Equation 2.14, where vx_n and vy_n are the components of the UAV's velocity vector which must be smaller than some ϵ_v .

$$cdone_n = cdone_{p,n} \wedge cdone_{v,n} \wedge \neg done_n \quad 0 \leq n < N \quad (2.13)$$

$$cdone_{v,n} = |vx_n| < \epsilon_v \wedge |vy_n| < \epsilon_v, \quad 0 \leq n < N \quad (2.14)$$

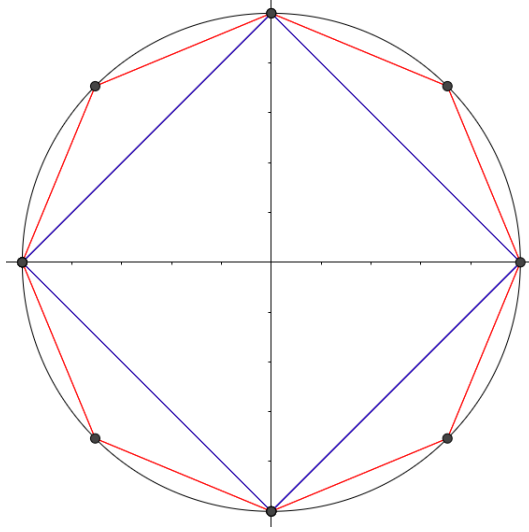


Figure 2.1: If the velocity is limited to a finite value, the velocity vector must lie within the circle centered on the origin with the radius equal to that value. This is represented by the black circle. This circle cannot be approximated in MILP, but it can be approximated using several linear constraints. The blue square shows the approximation using 4 linear constraints. The red polygon uses 8 linear constraints. As more constraints are used, the approximation gets closer and closer to the circle.

2.5 Vehicle state limits

Like any vehicle, a UAV has a certain maximum velocity. The model should contain constraints which prevent the UAV from moving faster than the maximum velocity. The magnitude of the velocity is the 2-norm of the velocity vector (which is Pythagoras' theorem for a 2D vector). This cannot be represented as a linear constraint because the components of the velocity vector need to be squared. However, the 2-norm can be approximated using multiple linear constraints.

Figure 2.1 visualizes how this works for the 2D case. All velocity vectors with a magnitude smaller than the maximum velocity are on the inside of the black circle with radius v_{max} . This cannot be expressed in MILP, but a regular polygon which fits inside the circle can be expressed. As the amount of vertices N_{vertex} making up the polygon increases, the approximation gets more and more accurate. The coordinates of the vertices of the polygon, $q_{x,i}$ and $q_{y,i}$ are defined by Equations 2.15-2.17 in counter-clockwise order.

$$\theta = \frac{2\pi}{N_{points}} \quad (2.15)$$

$$q_{x,i} = v_{max} * \cos(\theta i), \quad 0 \leq i < N_{points} \quad (2.16)$$

$$q_{y,i} = v_{max} * \sin(\theta i), \quad 0 \leq i < N_{points} \quad (2.17)$$

Like before, the equations are limited to the 2D case, but can be extended to 3D as well. Each edge of the polygon defines a line with slope a_i and intercept b_i , as determined by Equations 2.18-2.20.

$$\Delta q_{x,i} = q_{x,i} - q_{x,i-1}, \quad \Delta q_{y,i} = q_{y,i} - q_{y,i-1} \quad (2.18)$$

$$a_i = \frac{\Delta q_{y,i}}{\Delta q_{x,i}} \quad 0 \leq i < N_{vertex} \quad (2.19)$$

$$b_i = q_{y,i} - a_i q_{x,i} \quad 0 \leq i < N_{vertex} \quad (2.20)$$

Finally, the constraints can be constructed using the slope and intercepts of each line segment. For the edges on the "top" half of the polygon, the velocity vector must stay *below* those edges. This is expressed by Equation 2.21. Similarly, for the bottom half, the velocity vector must stay *above* those edges as expressed by Equation 2.22. If N_{vertex} is odd, the left-most edge of the polygon is vertical. Equation 2.23 handles this special case: the velocity vector must stay on the right of the left-most edge. TODO: add figure to explain better.

$$vy_n \leq a_i vx_n + b_i, \quad \Delta q_{x,i} < 0, \quad 0 \leq n < N \quad (2.21)$$

$$vy_n \geq a_i vx_n + b_i, \quad \Delta q_{x,i} > 0, \quad 0 \leq n < N \quad (2.22)$$

$$vx_n \geq q_{x,i}, \quad \Delta q_{x,i} = 0, \quad 0 \leq n < N \quad (2.23)$$

The acceleration and other vector properties of the vehicle can be limited in the same way.

2.6 Obstacle avoidance

The last element of the model is obstacle avoidance. Obstacles are regions in the world where the UAV is not allowed to be. This may be due to a physical obstacle, but it could also be a no-fly zone determined by law or other concerns.

Assuming that each obstacle is a 2D convex polygon, the constraints for obstacle avoidance are similar to those of the vehicle state limits in Section TODO:ref. However, the big difference is that the UAV must stay on the outside of the polygon instead of the inside.

2.6.1 Importance of Convexity

The maximum velocity is modeled without using any integer variables. This is possible because the allowed region for the velocity vector is a convex shape. A shape is convex if a line drawn between any two points inside that shape is also fully inside the shape. This is demonstrated in Figure 2.3a

This property does not hold for obstacle avoidance. If the UAV is on one side of an obstacle, it cannot move in a straight line to the other side of that obstacle. Because of that obstacle, the shape formed by all the positions where the UAV is allowed to

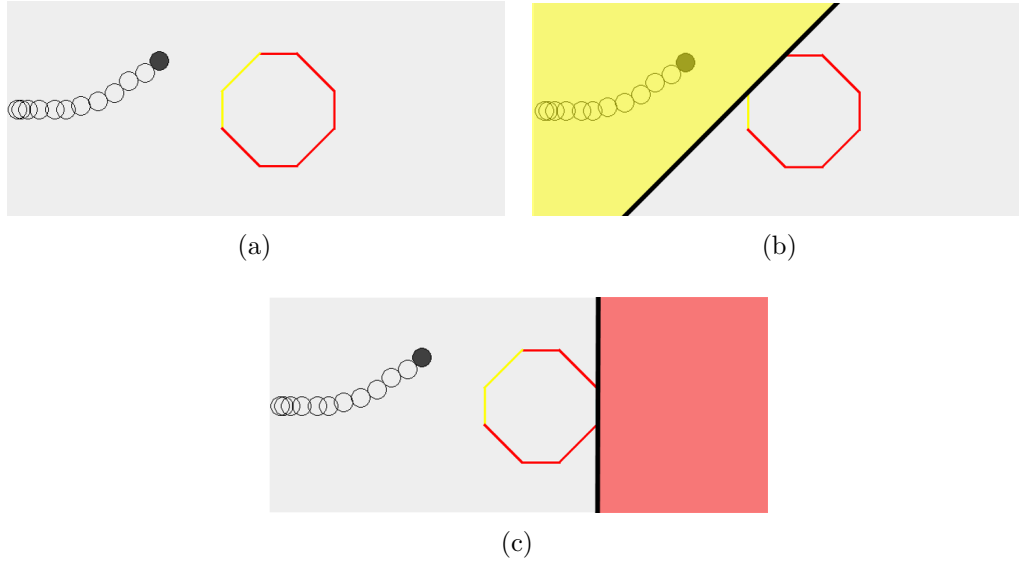


Figure 2.2: A visual representation of how obstacle avoidance works. The top image shows the vehicle's current position as the filled circle, with its path in previous time steps as hollow circles. The color of the edges of the obstacle represent whether or not the vehicle is in the safe zone for that edge. An edge is yellow if the vehicle is in the safe zone, and red otherwise. The middle image shows the safe zone defined by a yellow edge in yellow. Note how the vehicle is on one side of the black line and the obstacle is entirely on the other side. The bottom image shows an edge for which the vehicle is not in the safe zone (represented in red this time). As long as the vehicle is in the safe zone of at least one edge, it cannot collide with the obstacle.

convex

(a) TODO:convex

nonconvex

(b) TODO:nonconvex

be is no longer convex. This can be seen in Figure 2.3b.

To express non-convex constraints, integer variables are needed. This causes the difference between what can be modeled in Linear Programming versus Mixed-Integer Linear Programming: non-convex constraints can be expressed in MILP, while this is not possible in LP.

2.6.2 Big M Method

Like with the maximum velocity in Section 2.5, the edges of the obstacle are used to construct the constraints. Each edge defines a line, as determined by Equations 2.18-2.20. If the obstacle is convex, the obstacle will entirely on one side of that line. If the UAV is on the other side, the one without the obstacle, it cannot collide with that obstacle. This region can be consider the safe region defined by that edge. As long as the UAV is in the safe region of at least one edge, no collisions can occur. Figure 2.2 demonstrates this visually.

A popular way to model this is the "Big M" method TODO:cite. For each edge, a

constraint is constructed which forces the UAV to be in the safe region for that edge. However, the UAV must only be in the safe region of at least one edge. This means that it must be possible to "turn off" constraints.

For each edge of an obstacle, a boolean *slack* variable is used to represent whether or the constraint for that edge is enabled. If this *slack* variable is *true* (equal to 1), the constraint is *disabled*. This is where the "Big M" comes in: the *slack* variable is multiplied by a very large number M on one side of the inequality constraint for that edge. M must be chosen to be large enough to ensure that ,when *slack* is *true*, the inequality is always satisfied.

In Equations 2.24-2.27 below, $q_{x,i}$ and $q_{y,i}$ are the 2D coordinates of vertex i the obstacle. The slope a_i and intercept b_i of edge i are calculated as in Equations 2.18-2.20. For every time step n :

$$y_n + M * slack_{i,n} \geq a_i x_n + b_i, \quad \Delta q_{x,i} < 0 \quad (2.24)$$

$$y_n - M * slack_{i,n} \leq a_i x_n + b_i, \quad \Delta q_{x,i} > 0 \quad (2.25)$$

$$x_n - M * slack_{i,n} \leq q_{x,i}, \quad \Delta q_{y,i} < 0, \quad \Delta q_{x,i} = 0 \quad (2.26)$$

$$x_n + M * slack_{i,n} \geq q_{x,i}, \quad \Delta q_{y,i} > 0, \quad \Delta q_{x,i} = 0 \quad (2.27)$$

Like in Equations 2.21 and 2.22, edges on the top and bottom of the obstacle are treated differently. Equation 2.24 covers the top edges. The UAV must be above the edge. If the UAV is not above the edge (when y_n is too small), enabling $slack_{i,n}$ will add M on the left-hand side of the inequality and ensure that it is always larger than the right-hand side. Equation 2.25 does the same for edges on the bottom. The inequality is flipped around so that the UAV must be below the edge. This also means that M must be subtracted from the left-hand side of the inequality to ensure the constraint is always satisfied.

Vertical edges are also possible. A vertical edge may occur on the left or right side of the polygon, as covered in Equations 2.26 and 2.27 respectively.

Finally Equation 2.28 ensures that at least one of the slack variables must be false at each time step.

$$\neg \bigwedge_i slack_{i,n} \quad 0 \leq n \leq N \quad (2.28)$$

Equations 2.24 - 2.27 assume that the UAV has no physical size. The position of the UAV is the position of its center of mass. Because a UAV has certain physical dimensions, it will collide with an obstacle before its center of mass reaches the obstacle. The vehicle's shape is approximated as a circle with radius r . The vertical offset v_i required to move the line with slope a_i from the center of the circle to the edge is calculated by Equation 2.29. A geometric proof is given in Figure 2.4.

$$v_i = r \sqrt{1 + a_i^2} \quad (2.29)$$

With the vertical offset calculated, Equations 2.24 - 2.27 can be extended to Equations 2.30-2.31 which take the UAV size into account.

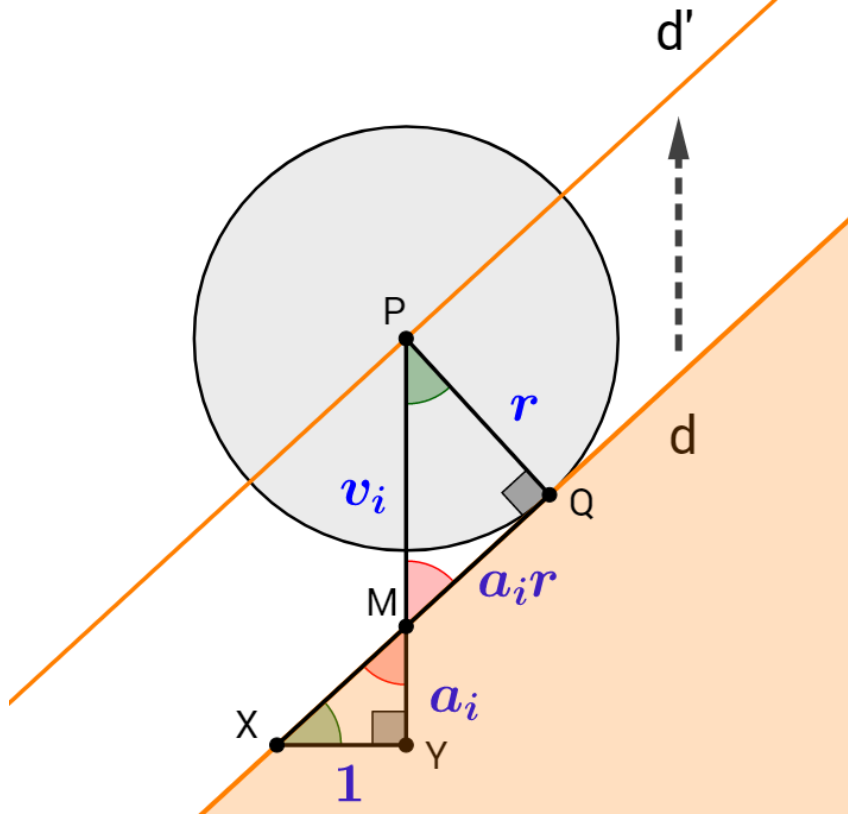


Figure 2.4: A geometric proof for the vehicle offset formula in Equation 2.29. Measures are marked in blue. P is the center of mass of the UAV. d is the line defined by edge i of an obstacle. The obstacle is the orange region. We wish to translate d vertically to d' such that when the UAV's center of mass P touches d' , the circle with radius r (representing the UAV's shape, colored in grey) touches d in Q . If d' is used for the constraint instead of d , the UAV cannot collide with the obstacle. The difference between the intercepts of d and d' is $v_i = |PM|$. The slope of d' is a_i , so if XY is horizontal and $|XY| = 1$, then $|MY| = a_i$. Corner M is the same in both triangle PQM and XYM , as marked in red. Corner Q and Y are both right angles. This means PQM and XYM are similar triangles. As a result: if $|PQ| = r$, then $|QM| = a_i r$. Using Pythagoras' theorem: $v_i = \sqrt{r^2 + a_i^2 r^2} = r\sqrt{1 + a_i^2}$.

$$y_n + M * slack_{i,n} - v_i \geq a_i x_n + b_i, \quad \Delta q_{x,i} < 0 \quad (2.30)$$

$$y_n - M * slack_{i,n} + v_i \leq a_i x_n + b_i, \quad \Delta q_{x,i} > 0 \quad (2.31)$$

$$x_n - M * slack_{i,n} + r \leq q_{x,i}, \quad \Delta q_{y,i} < 0, \quad \Delta q_{x,i} = 0 \quad (2.32)$$

$$x_n + M * slack_{i,n} - r \geq q_{y,i}, \quad \Delta q_{y,i} > 0, \quad \Delta q_{x,i} = 0 \quad (2.33)$$

Segmentation of the MILP problem

3.1 Algorithm approach

The MILP model described in section 2 is sufficient to solve the trajectory planning problem for short flights with few obstacles. However, it scales poorly when the duration of the flight or the amount of obstacles is increased. Mixed-Integer programming belongs to the “NP-Complete” class of problems [?]. Assuming there are n boolean variables, the worst case complexity is $O(2^n)$. An boolean variable is needed for every edge of every polygon, for every time step. By reducing both the amount of time steps needed and obstacles that need to be modeled, the execution time can be reduced dramatically.

The key insight that allows my algorithm to scale well beyond what’s usually possible is that the path trajectory not need to be solved all at once. If the trajectory planning problem can be split into many different subproblems, each subproblem becomes easier to solve. The solution for each subproblem is a small part of the final trajectory. By solving theses subproblems sequentially, the final trajectory can gradually be constructed.

While diving the problem into subproblems does make things much easier to solve, it also has an important down side: Finding the fastest trajectory can no longer be guaranteed. Smaller subproblems make it easier to find a solution, but fundamentally the problem of finding the optimal trajectory is still just as hard. The necessary trade-off for better performance is that the optimal trajectory will likely not be found. Luckily, the optimal trajectory is often not required in navigation. A reasonably good trajectory will do.

3.1.1 The importance of convexity

While the worst case time needed to solve a MILP problem increases exponentially with the amount of integer variables, this is not the most useful way to measure the difficulty of a problem. Modern solvers are heavily optimized and are able to solve certain problems with many integer variables much faster than others. The key difference is the convexity of the solution space. Just like a circle is the solution space for “all points a certain distance away from the center point”, the constraints used to model the trajectory planning problem form some geometric shape with a dimension for every variable.

When only linear constraints with real values are used, the solution space will always be convex. It is this convexity that makes a standard linear program easy to solve. When integer variables are introduced, it is possible to construct solution spaces which are not convex. As the solution space becomes less and less convex, the problem becomes harder to solve. Integer variables can be seen as a tool which allows non-convex solution spaces to be modeled. When trying to improve the difficulty of a problem, the actual goal is making the problem more convex (or smaller, which always helps). Reducing the amount of integer variables is only a side effect. This insight is critical when determining how to divide the trajectory problem into smaller subproblems, and which obstacles are important for each subproblem.

3.1.2 General Algorithm Outline

Algorithm 1 General outline

```

1:  $T \leftarrow \{\}$  ▷ The list of solved subtrajectories
2:  $path \leftarrow \text{THETA}^*(scenario)$ 
3:  $events \leftarrow \text{FINDTURN}EVENTS(path)$ 
4:  $segments \leftarrow \text{GEN}SEGMENTS(path, events)$ 
5: for each  $segment \in segments$  do
6:    $\text{UPDATE}STARTSTATE(segment)$ 
7:    $\text{GEN}SAFEREGION(scenario, segment)$ 
8:    $\text{GEN}SUBMILP(scenario, segment)$ 
9:    $T \leftarrow T \cup \{ \text{SOLVE}SUBMILP \}$ 
10: end for
11:  $result \leftarrow \text{MERGE}TRAJECTORIES(T)$ 

```

Algorithm 1 shows the general outline of the algorithm. It consists of two phases. The first phase gathers information about the trajectory planning problem. A Theta* path planning algorithm is used to find an initial path (line 2). From this initial path, turn events are generated (line 3). These turn events mark where the trajectory will have to turn.

The second stage builds and solves "segments". Each segment represents a single sub-trajectory. The segments contain the information needed to build the corresponding MILP subproblem, which can in turn be solved by the solver. First, each segment is generated (line 3) from the turns found in the previous step. Before the MILP subproblem can be generated and solved (line 8-9), a heuristic selects several obstacles to be modeled in the problem. A genetic algorithm generates a safe region which is allowed to overlap those selected obstacles only (line 7). To ensure a seamless transition between two consecutive sub-trajectories, the starting state for the UAV in the MILP current segment is updated to match the final state of the UAV in the previous segment (line 6). Finally, the sub-trajectories are merged together to form the final trajectory (line 11).

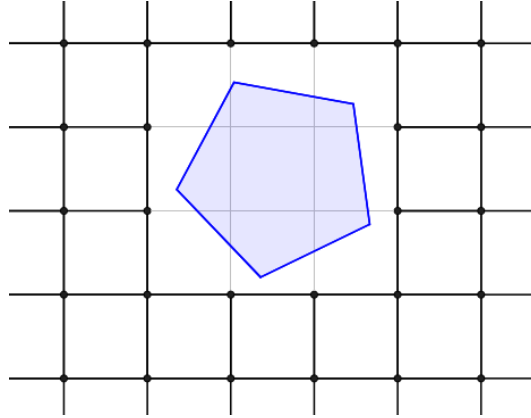


Figure 3.1: An example of how a grid is used to build the graph for the path finding algorithm. Each point is a node on the graph. If two points are connected by a line, their nodes in the graph also are connected by an edge. Diagonal edges are not shown here for clarity.

3.2 Finding the initial path

The first step in Algorithm 1 is finding the Theta* path (line 2). This path will be used to divide the trajectory planning problem into segments. The MILP-problem generated from each of those segments needs an intermediate goal to get the UAV closer to the final goal position. These intermediate goals will be determined by the Theta* path.

This path is not only useful to guide the trajectory towards the goal. It is also lets the algorithm determine where the turns will be in the trajectory. reason!!!

3.2.1 A*

Theta* is a variant of the A* path planning algorithm. In A*, the world is represented as a graph. Each possible position is represented as a node, with edges between nodes if one position can be reached from the other. The distance between connected positions is represented as a weight or cost on each edge.

Planning a path consists of picking a start and goal node. The A* algorithm will traverse the edges between nodes, keeping track of which edges it traversed to reach a certain node. When the algorithm reaches the goal node, the nodes visited to reach that goal node are the path from the start node to the goal .

In this case, the world the UAV travels through is a continuous (2D) world. The graph for A* star is generated by overlaying a grid on the world. Nodes are placed at each intersection of the grid, as long as they are not inside obstacles. Each node is also connected to its neighbors by moving horizontally, vertically or diagonally along the grid. Figure ?? shows an example of this.

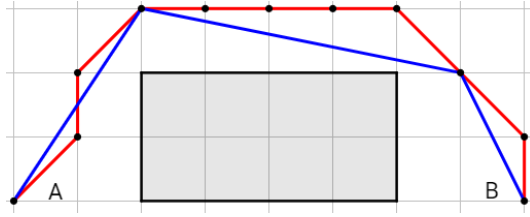


Figure 3.2: The red line shows a typical A* path, compared to the path found by Theta*. The gray rectangle is an obstacle.

3.2.2 Reason for Theta*

A* finds the shortest path through the graph. However, this graph is only an approximate representation of the actual continuous world. An A* path will only travel along the edges of the graph. This means that the path can only travel horizontally, vertically and possibly diagonally. If the shortest path between two points is at another angle, the A* path will contain zig-zags or detours because it is limited to traveling along the grid.

Theta* solves this problem. It is nearly identical to A*, but it allows the path to travel at arbitrary angles. It still traverses the graph using the edges between nodes, but does not restrict the path to only following those edges.

3.2.3 Theta* implementation

TODO: paraphrased! CITE!! Algorithm 2 shows how Theta* is implemented. It uses the following elements:

- the g-value $g(s)$ is the length of the shortest path between the start node and s .
- a function $c(s, s')$ which returns the distance between node s and s' .
- a heuristic function $h(s)$, which approximates the path distance left before the goal position s_{goal} is reached. The straight line distance between s and the s_{goal} is used, such that $h(s) = c(s, s_{goal})$. An admissible heuristic function must always be an underestimation of the actual path distance to the goal, which is ensured by using the straight line distance.
- a function $parent(s)$ which returns the node before s in the path. When the parent of a node is *null*, it is either not part of the path or the first node of the path.
- a priority queue *queue*. This is a queue of nodes to expand next. Each node s is added with a value x using the *queue.Insert(s, x)* method. If s is already in *queue*, its value is updated to x . The *queue.Pop()* method removes and returns the node s with the lowest value x .
- a set *expanded* which contains all nodes which have already been expanded.

Algorithm 2 Theta* Implementation

```
1: function THETA*(scenario)
2:    $g(v_{start}) \leftarrow 0$ 
3:    $parent(v_{start}) \leftarrow null$ 
4:    $queue \leftarrow \emptyset$ 
5:    $queue.Insert(v_{start}, g(v_{start}) + h(v_{start}))$ 
6:    $expanded \leftarrow \emptyset$ 
7:   while  $queue \neq \emptyset$  do
8:      $s \leftarrow queue.Pop()$ 
9:     if  $s = v_{goal}$  then
10:       return  $s.GetPath()$ 
11:     end if
12:      $expanded \leftarrow expanded \cup \{s\}$ 
13:     for each  $s' \in \text{GenerateNeighbors}(s)$  do
14:       if  $s' \notin expanded$  then
15:          $UpdateVertex(s, s')$ 
16:       end if
17:     end for
18:   end while
19:   return "no path found"
20: end function
21: function UPDATEVERTEX( $s, s'$ )
22:   if  $LineOfSight(parent(s), s')$  then
23:      $s_{parent} \leftarrow parent(s)$ 
24:   else
25:      $s_{parent} \leftarrow s$ 
26:   end if
27:   if  $g(s_{prev}) + c(s_{prev}, s') < g(s')$  then
28:      $g(s') \leftarrow g(s_{parent}) + c(s_{parent}, s')$ 
29:      $parent(s') \leftarrow s_{parent}$ 
30:      $queue.Insert(s', g(s') + h(s'))$ 
31:   end if
32: end function
```

- a function `GenerateNeighbors(s)` which generates and returns the neighbors of node s . These are the neighboring positions on the grid around s

Initialization When the algorithm initializes, the g-value of the start node v_{start} is set to zero and its parent is set to *null* (line 2-3). The priority queue *queue* is initialized, and v_{start} is added to it with value $g(v_{start}) + h(v_{start})$. The value attached to a node v in the priority queue is the shortest possible length of a path going from the start v_{start} to the goal v_{goal} , while going through v . The g-value is the length of the path between v_{start} and v , while $h(s)$ is an estimate of the length of the path between v and v_{goal} .

Main loop `queue.Pop()` always removes the node with s the lowest value (line 8). This means that as more nodes get added to *queue*, the algorithm will always explore the "most promising leads" first. If $s = v_{goal}$, the goal has been reached and the path is returned (line 9-11). Otherwise, s is added to *expanded* (line 12). This prevents s from being added to *queue* again. Line 13 generates every neighbor s' of s according to the grid and obstacles, as seen in Figure ??, "expanding" node s . If the neighbor s' has not been expanded yet, `UpdateVertex(s, s')` is called (line 14-16).

UpdateVertex So far, the algorithm is identical to A*. The only difference between A* and Theta* are lines 22-26. Line 22 checks if the parent of s , which is the node before s in the path, can be connected in a straight line to s' . Going from $parent(s)$ to s' directly is always shorter than going from $parent(s)$ to s and from s to s' due to the triangle inequality. If $parent(s)$ and s' are in line of sight, the path should be constructed from $parent(s)$ to s' , skipping s . Otherwise, the path goes through s , which is the behavior of A*. The choice of which node should be parent of s' is stored as s_{parent} .

Line 27 checks if the path through s_{parent} to s' is the shortest path to s' found so far. If this is not the case, a shorter path to s' exists so the path through s_{parent} can safely be ignored. Otherwise, the g-value of s' is updated to the length of the path to s_{parent} , $g(s_{parent})$ plus the distance between s_{parent} and s' , $c(s_{parent}, s')$ (line 28). The shortest path to s' is updated by setting $parent(s')$ to s_{parent} (line 29). Finally, s' is added to *queue* to be expanded further.

3.2.4 Performance improvements

By introducing the line of sight check, Theta* is considerably slower than A* in large worlds with many obstacles. The goal of this thesis is to improve scalability of trajectory planning to large and complex worlds, so the preprocessing phase must also scale well.

To help Theta* scale, the world is divided into rectangular sectors. When the world is first loaded, the algorithm determines in which sector(s) each obstacle is placed, creating an index mapping sectors to obstacles.

When the line of sight check is executed, the algorithm determines which sectors the line crosses. This is usually just one or two sectors. By using the index, only the

obstacles in those sectors need to be considered for the line of sight check. This is much faster than having to check every obstacle in the entire world every time.

3.3 Detecting turn events

According to Hypothesis 1, the degree of non-convexity around the trajectory is responsible for the poor performance of MILP trajectory planning problem. This local degree of non-convexity around the trajectory is the amount of distinct convex shapes the trajectory needs to pass through to reach the goal position, such that every point in the trajectory lies within at least one shape.

Within a single convex shape, by definition, it is always possible to move in a straight line from one side of the shape to the other. As a consequence, if multiple convex shapes are needed, the trajectory needs to make a turn. If the turn is not needed, that implies the trajectory can go in a straight line, which means that only a single convex shape is needed.

Because of this, the turns in the trajectory and the degree of non-convexity are directly related. Every turn in the trajectory is a manifestation of a transition between two or more convex shapes, and thus contributes to the degree of non-convexity of the entire trajectory.

Solving the trajectory in smaller segments reduces the degree of non-convexity in each segment, making them easier to solve. If Hypothesis 1 is true, minimizing the amount of turns in each segment will improve performance even more.

While the Theta* path is only a rough approximation of the trajectory, it does have turns in roughly the same places as the trajectory will have. Finding those turns allows the algorithm build segments such that the amount of turns in each segment is minimal.

Because Theta* is used to generate the initial path, finding the turns is easy. When two nodes are in each other's line of sight, it is possible to construct a convex shape around those points. When they are not within line of sight, which is when Theta* keeps the previous node in the path, this is not possible. Using the same reasoning as above, the nodes in the Theta* path must always coincide with turns in both the Theta* path and the trajectory.

While every node in the Theta* path (except the start and goal) coincide with a turn, they can be close together. When two or more consecutive nodes turn in the same direction (clockwise or counter-clockwise) and are close enough together, they can be considered to represent a single turn. The algorithm groups those nodes together in a turn event. Each turn event contains one or more nodes. A turn event predicts the existence of a turn in the MILP trajectory based on the Theta* path, bridging the gap between them.

3.3.1 Algorithm Implementation

Algorithm 3 processes the Theta* path to generate turn events. Two factors determine whether or not nodes are grouped together into events:

- The turn direction: a node v in the path can either turn the path clockwise or counter-clockwise, as determined by $\text{TURN DIR}(v)$. Two nodes with a different turn direction cannot be in the same turn event
- The maximum distance between two nodes in a turn event: Nodes which are too far from each other should not be merged. This distance Δ_{max} is based on a turn tolerance parameter multiplied by the UAV's maximum acceleration distance (MAD).

Maximum Acceleration Distance With a_{max} and v_{max} respectively the UAV's maximum acceleration and velocity, the time needed to reach the maximum velocity is $t_{max} = v_{max}/a_{max}$. The maximum acceleration distance in the distance traveled in that time, which is $t_{max}^2/2 = v_{max}^2/2a_{max}$. The MAD is used in several places in the algorithm as an approximation of the distance in which the UAV can recover from a maneuver. In $1 * MAD$, the UAV can accelerate to any velocity from zero, or it can stop from any velocity. In $2 * MAD$, the UAV can transition from any velocity vector to any other velocity vector. It is an approximation of the distance at which the presence or absence of an event can influence the UAV.

In this case, the MAD is relevant because turns require the velocity vector of the UAV to change from before the turn to after the turn. If two nodes have a distance of more than $2 * MAD$ between them, the turns at each node can be taken independently as distinct turns. TODO: fig!

In the Theta* path, all but the first and last nodes are turns in the path. The second node is always the first node in a new turn event (line 5). Subsequent nodes in the path which are not too far away from the previous node (line 9) and turn in the same direction (line 12) are added to the current turn event (line 15). The maximum distance between nodes in the same turn is Δ_{max} . Once a node is found which does not belong in the event, the event is stored (line 18), a new event is created for that node (line 5) and the process repeats until no more nodes are left.

3.4 Generating path segments

Once the turn events are found, the next step is generating the segments. Each segment defines a single MILP problem whose solution is a small part of the desired trajectory. As argued above, each turn event should be solved in a separate MILP problem to keep the solve times low.

Algorithm 4 calculates the boundaries of the segments, based on the Theta* path and the turn events. For the best performance, these segments should be as small as possible. However, performance is not the only factor. Stability of the algorithm is also important. Each segment needs to be large enough so the UAV can safely approach and exit each turn. This can be guaranteed by ensuring a segment always starts at least the maximum acceleration distance (MAD) before the turn event. The distance between the start of the segment and the turn event in that segment is called the expansion distance. When the expansion distance is least $1 * MAD$, the

Algorithm 3 Finding Turn Events

```

1: function FINDTURNEvents(path)
2:    $\Delta_{max} \leftarrow \text{max. acc. distance} * \text{turn tolerance}$ 
3:   events  $\leftarrow \{\}$  ▷ The list of turn events found so far
4:   i  $\leftarrow 1$  ▷ Skip the start node, it can't be a turn
5:   while i < |path| - 1 do ▷ Skip the goal node
6:     event  $\leftarrow \{\text{path}(i)\}$  ▷ Start new turn event
7:     turnDir  $\leftarrow \text{TURNDir}(\text{path}(i))$ 
8:     i  $\leftarrow i + 1$ 
9:     while i < |path| - 1 do
10:      if ||path(i - 1) - path(i)|| >  $\Delta_{max}$  then
11:        break ▷ Node is too far from previous
12:      end if
13:      if TURNDir(path(i))  $\neq$  turnDir then
14:        break ▷ Node turns in wrong direction
15:      end if
16:      event  $\leftarrow \text{event} \cup \{\text{path}(i)\}$  ▷ Add to event
17:      i  $\leftarrow i + 1$ 
18:    end while
19:    events  $\leftarrow \text{events} \cup \{\text{event}\}$ 
20:  end while
21:  return events
22: end function

```



Figure 3.3: The left image shows the results after the Theta* algorithm has executed. The blue shapes are obstacles, while the gray line is the Theta* path. The right image shows the results after the path is segmented. Extra nodes have been added to the Theta* path, as marked by the green circles. These circles depict the transitions between segments.

UAV can come to a complete stop before it reaches the turn. If the UAV can safely come to a stop, it can also slow down to an appropriate speed to safely navigate the turn. Extending the segment beyond the end of the turn event also ensures that the



Figure 3.4: The left image shows the result after the genetic algorithm has executed. The obstacles in red have been selected to be modeled in the MILP problem. The dark grey shape is the convex allowed region generated by the genetic algorithm. Note how it does not overlap with any of the blue obstacles. The right image shows the final result. The trail of circles show the path of the vehicle up to the current time step, which is represented by the filled circles. The red and yellow colors depict the same information as in figure 2.2

UAV must have completely navigated the turn by the end of the segment. Ensuring that the UAV can always safely navigate a turn means that the MILP solver can always find a feasible trajectory for that segment. Because of this, ensuring safety also ensures stability.

Increasing the approach margin beyond the minimum required for stability can improve the speed of the trajectory. An approach margin of $1 * MAD$ is considered safe because the UAV can still "slam on the breaks" to slow down in time for the turn. However, a larger expansion distance gives the UAV more time and space to maneuver so it can efficiently navigate the turn. The ratio between the expansion distance and the MAD is called the approach margin: $expansiondistance = approachmargin * MAD$. Since the MAD is determined by the UAV's properties, the approach margin is used as the parameter which controls the expansion distance.

3.4.1 Implementation

To generate the segments, Algorithm 4 considers each turn event in turn (line 5-6). *lastEnd* is always the end of the last segment that has been generated. It is initialized with the start position of the UAV (line 4). The algorithm considers turn events, but consecutive turn events may have a large distance between them. In those cases, additional segments (straight, without turns) may need to be generated to "catch up" with the start of the turn events. When straight segments need to be inserted, the *catchUp* flag is set to *true*. *catchUp* starts as *true* to catch up from the start position of the UAV to the first turn event (line 3).

First, consider the case in which there is no need to catch up to generate the segment for turn event i . The start of the segment is the end of the last segment,

Algorithm 4 Generating the segments

```

1: function GENSEGMENTS(path, events)
2:   segments  $\leftarrow \{\}$ 
3:   catchUp  $\leftarrow \text{true}$ 
4:   lastEnd  $\leftarrow \text{path}(0)$ 
5:   for  $i \leftarrow 0, |events| - 1$  do
6:     event  $\leftarrow \text{events}(i)$ 
7:     if catchUp then
8:       EXPANDBACKWARDS(event.start)
9:       ADDSEGMENTS(lastEnd, event.start)
10:      lastEnd  $\leftarrow \text{event.start}$ 
11:    end if
12:    nextEvent  $\leftarrow \text{events}(i + 1)$ 
13:    if nextEvent.start is close to event.end then
14:      mid  $\leftarrow$  middle between event & nextEvent
15:      ADDSEGMENTS(lastEnd, mid)
16:      lastEnd  $\leftarrow \text{mid}$ 
17:      catchUp  $\leftarrow \text{false}$ 
18:    else
19:      EXPANDFORWARDS(event.end)
20:      ADDSEGMENTS(lastEnd, event.end)
21:      lastEnd  $\leftarrow \text{event.end}$ 
22:      catchUp  $\leftarrow \text{true}$ 
23:    end if
24:  end for
25:  ADDSEGMENTS(lastEnd, path( $|path| - 1$ ))
26:  return segments
27: end function

```

lastEnd. The desired end of the segment is found by expanding the end of the turn event forwards along the path by a distance equal to the expansion distance. However, This may not be possible or desirable if the next turn event ($i + 1$) is too close. Two events are considered close to each other if they are separated by less than three¹ times the expansion distance (line 13).

When the current turn event and the next are too close, the middle *mid* between those turn events is used as the boundary between the segments. In this case, the current segment is generated from *lastEnd* to *mid* (line 14-16). The next turn event is nearby, so there is no need to catch up (line 17).

When there is plenty of distance between the current turn event and the next, this is not necessary. The end of the turn event *event.end* can be expanded forwards along the path by the full expansion distance (line 19-21). There is some distance between

¹Requiring three (instead of two) times the expansion distance as separation between turn events ensures that the segment between those turns is also at least as long as the expansion distance. This prevents some issues that can occur with very short segments.

this turn event and the next, so catching up will be required before the next event (line 22).

Before each turn event is considered, the algorithm checks if it needs to catch up first (line 7). If so, the start of the turn event is expanded backwards along the path by the desired expansion distance (line 8). One or more straight segments are added between the end of the last segment *lastEnd* and the (backwards expanded) start of the current event *event.start* (line 9-10). There are no turns in those straight segments, so their size can be kept small without the risk for stability issues.

3.4.2 Amount of time steps

The amount of time steps in the MILP problem needs to be determined ahead of time. The length of the Theta* path is used to estimate how much time is needed for the UAV to reach the end of each segment. To ensure that there are always enough time steps, a conservative estimate is used. This estimate assumes that the UAV starts the segment while stopped. Afterwards, the UAV accelerates towards the turn in the segment and comes to a stop at the turn. Finally, the UAV accelerates again from the turn and stops again at the end of the segment. The time needed to complete those actions is multiplied by a multiplier parameter.

3.5 Generating the active region for each segment

The last step of preprocessing determines which obstacles will be modeled in the MILP problem for each segment. Segmentation already reduces both the amount of time steps needed and the nonconvexity in each segment. However, modeling a large amount of obstacles still reduces the performance to unacceptable levels.

Not every obstacle needs to be modeled in the MILP subproblems to avoid collisions. Only the obstacles in the neighborhood around each segment are relevant.

Furthermore, not all obstacles in the neighborhood actually need to be modeled either. There is a fundamental difference between the obstacles on the inside of the turn and those on the outside. Obstacles on the inside of a turn are the "cause" for that turn. They cause the non-convexity around the trajectory. Without those obstacles, the UAV could move in a straight line in a convex neighborhood. Obstacle avoidance for the inner obstacles must reduce convexity

The same is not true for obstacles on the outside of the turn. Without those obstacles the optimal trajectory may have a slightly different shape, but the turn would still be there. As a result, obstacle avoidance for the outer obstacles does not necessarily have to reduce convexity.

Figure 3.5 shows this difference. The UAV cannot collide with obstacles on the outside of the turn as long as it stays inside the colored convex polygon. As long as this convex polygon does not overlap any of the obstacles on the outside of the corner and the UAV is constrained to stay within the polygon, those obstacles do not need to be modeled in the MILP problem. Only the few obstacles on the inside

Figure 3.5: genetic convexity example

of the turn will be modeled.

The obstacles to be modeled in the MILP problem are selected by calculating the convex hull of several important points of the segment. The algorithm use These are the start position, goal position and all nodes on the Theta* path between them. (TODO: more detail?). Any obstacle which overlaps this convex hull is on the inside of the turn and will be modeled in the MILP problem. In some cases, obstacles on the outside of the turn can be very restrictive. Due to the inherent randomness of the genetic algorithm, modeling those restrictive obstacle in the MILP problem as well improves stability.

The convex hull can be considered a safe region. If the UAV stays inside this region, it cannot collide with obstacles since any obstacle that overlaps with the safe region is modeled in the MILP problem. However, this safe region restricts the movements of the UAV more than necessary.

To make the safe region less restrictive, we use a genetic algorithm which attempts to grow it. TODO: FIG.

3.5.1 Implementation of the genetic algorithm

A genetic algorithm is an algorithm which evolves solutions using a process inspired by natural selection in biological evolution. Genetic algorithms typically use a population of individuals which compete with each other. Each individual has a genome consisting of chromosomes, which in turn consist of individual genes. The genome determines the traits of each individual, also called the phenotype. The structure and quantity of the genes depends on the kind of problem that the genetic algorithm should solve.

Like in biology, the individuals can produce offspring. This offspring can be a crossover between multiple parent individuals, or a mutated version of a single parent. An important part of evolution is the concept of "survival of the fittest". A genetic algorithm improves its population by letting individuals compete. The losing individuals get eliminated from the population, while those who remain get the opportunity to create offspring. This competition is based on a fitness function. Each individual represents a possible solution for a problem. The fitness function scores the individuals based on how well they solved the problem.

Algorithm 5 shows the implementation of the genetic algorithm. In this implementation, each individual in the population represents a single legal polygon. A legal polygon is convex, does not self-intersect, can only overlap with the selected obstacles and contains every node in the Theta* path for that specific segment. The latter requirement prevents the polygon from drifting off. Each individual has a single chromosome, and each chromosome has a varying number of genes. Each gene represents a vertex of the polygon.

The only operator is a mutator (line 4). Contrary to how mutators usually work, the

Algorithm 5 Genetic Algorithm

```

1: function GENSaFERegion(scenario, segment)
2:   pop  $\leftarrow$  SEEDPOPULATION
3:   for  $i \leftarrow 0, N_{gens}$  do
4:     pop  $\leftarrow pop \cup \text{MUTATE}(pop)$ 
5:     EVALUATE(pop)
6:     pop  $\leftarrow \text{SELECT}(pop)$ 
7:   end for
8:   return BESTINDIVIDUAL(pop)
9: end function
10: function MUTATE(pop)
11:   for each individual  $\in pop$  do
12:     add vertex with prob.  $P(\text{add vertex})$ 
13:     OR remove vertex with prob.  $P(\text{remove vertex})$ 
14:     for each gene  $\in individual.chromosome$  do
15:       randomly nudge vertex
16:       if new polygon is legal then
17:         update polygon
18:       else
19:         try again at most  $N_{attempts}$  times
20:       end if
21:     end for
22:   end for
23:   return BESTINDIVIDUAL(pop)
24: end function

```

mutation does not change the original individual. This means that the every individual can be mutated in every generation, since there is no risk of losing information. This mutator can add or remove vertices of the polygon by adding or removing genes (lines 12-13), but only if the amount of genes stays between a specified minimum and maximum. The mutator attempts to "nudge" every vertex/gene to a random position inside a circle around the current position (line 15). If the resulting polygon is not legal, it retries a limited number of times (line 16-19).

Tournament selection is used as the selector, with the fitness function being the surface area of the polygon (line 5-6). Fig. ?? Shows the obstacles modeled in the MILP problem in yellow and red, as well as the polygon generated by the genetic algorithm in dark gray.

Extensions

4.1 Solver-specific improvements

The main principles that drive the algorithm work regardless of which solver is used. However, the implementation can be improved by using more specific features of the solver. For this thesis, IBM CPLEX is used as the MILP solver. This is one of the fastest, proprietary solvers available on the market.

4.1.1 Indicator constraints

The Big M method to turn constraints on or off is functional, but there are some issues with it. M has to be big enough so it can always "overpower" the rest of the inequality. If M is too low, incorrect behavior may occur. However, if M is very large, CPLEX may have numerical difficulties or even find incorrect results ¹.

Indicator constraints are a solution for this problem. The goal of the large M is to overpower the inequality so the constraint can be turned on or off based on a boolean variable. Indicator constraints allow constraints to be turned on or off, based on other constraints. They provide a direct way to model an "if/then" relation. Equation 4.1 is a modified version of the obstacle avoidance constraints 2.30 - 2.33. If $slack_{i,n}$ is not true, then the matching constraint on the right side must be true.

$$\neg slack_{i,n} \rightarrow \begin{cases} y_n - v_i & \geq & a_i x_n + b_i, & \Delta q_{x,i} < 0 \\ y_n + v_i & \leq & a_i x_n + b_i, & \Delta q_{x,i} > 0 \\ x_n + r & \leq & q_{x,i}, & \Delta q_{y,i} < 0, & \Delta q_{x,i} = 0 \\ x_n - r & \geq & q_{y,i}, & \Delta q_{y,i} > 0, & \Delta q_{x,i} = 0 \end{cases} \quad (4.1)$$

4.1.2 Max time

When the MILP problem is sufficiently difficult to solve, it may take a long time before the solver can find the optimal solution. To ensure an upper limit on computation time, CPLEX accepts a maximum solve time parameter. When the maximum time has expired, it will return the best solution found so far.

In the experiments, the maximum solve time was typically 120 seconds per segment.

¹<http://www-01.ibm.com/support/docview.wss?uid=swg21400084>

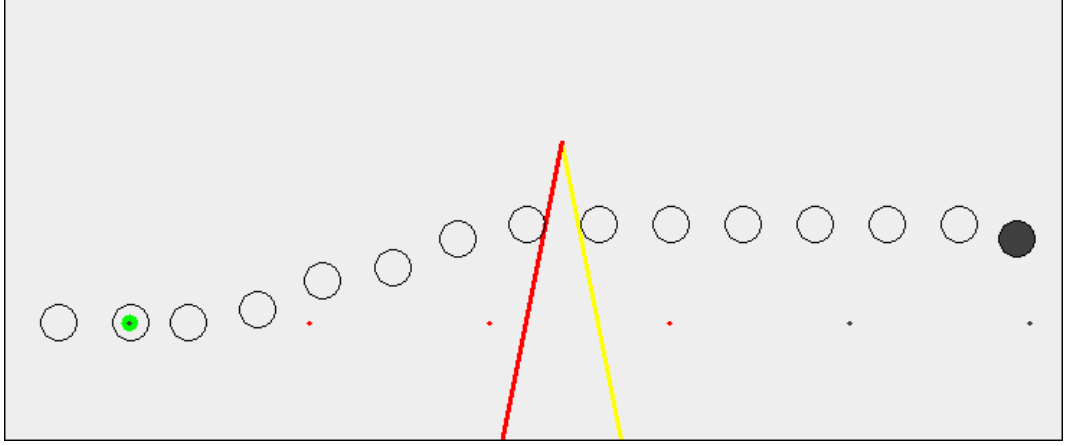


Figure 4.1: An example of corner cutting

The goal is for every segment to be relatively easy to solve, so if no solution can be found in two minutes it counts as a failure.

4.1.3 Max delta

During testing it became clear that the solver often spends a relatively long time trying to improve trajectories which are already nearly optimal, or optimal but not yet proven to be optimal. CPLEX provides a maximum delta parameter. The delta is the difference between the best solution found so far and the upper bound for the optimal solution. If the delta is below this maximum delta, the solvers stop executing and returns the best result. When this value is small, this can reduce some of the execution time while barely changing the quality of the trajectory.

4.2 Corner cutting

The MILP problem uses discrete time steps to model the changes in the UAV's state over time. An issue with this approach is that constraints are only enforced at those specific time steps. This allows the UAV to cut corners or even move through obstacles entirely if the vehicle is moving fast enough. Figure 4.1 shows an example of this. Each time step on its own is a valid position, but a collision is ignored between the time steps.

Using the indicator constraint notation, Equation 4.2 and 4.3 prevent collisions with obstacle o at time step n . Each edge of each obstacle has an associated *slack* variable, which determines whether or not the UAV is on the safe side for that edge.

$$\neg slack_{i,n} \rightarrow \begin{cases} y_n - v_i & \geq & a_i x_n + b_i, & \Delta q_{x,i} < 0 \\ y_n + v_i & \leq & a_i x_n + b_i, & \Delta q_{x,i} > 0 \\ x_n + r & \leq & q_{x,i}, & \Delta q_{y,i} < 0, & \Delta q_{x,i} = 0 \\ x_n - r & \geq & q_{y,i}, & \Delta q_{y,i} > 0, & \Delta q_{x,i} = 0 \end{cases} \quad (4.2)$$

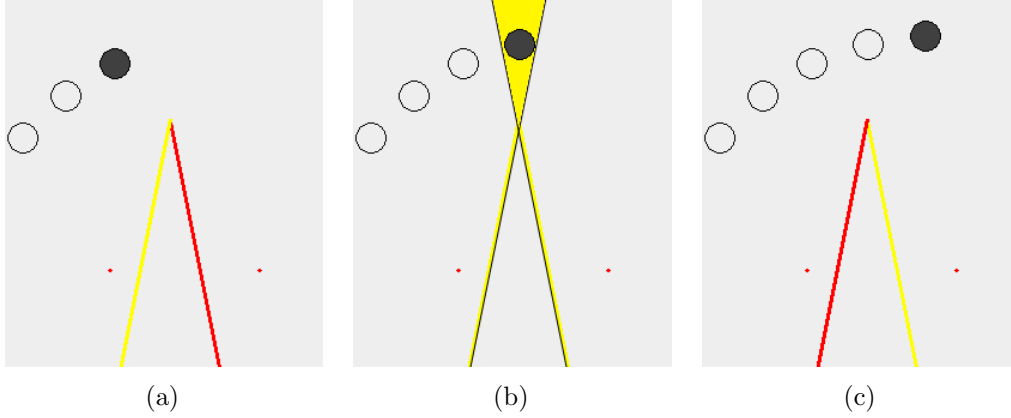


Figure 4.2: These images are three consecutive time steps which demonstrate how the corner cutting prevention works. In 4.2a, the UAV is in the safe region of the left edge (which is indicated by the yellow color). In 4.2c, the UAV is in the safe region for the right edge, but not the left edge. To ensure that the UAV does not cut the corner, the UAV must enter the safe region of the right edge before it exits the safe region of the left edge. The intersection between those two safe regions is the inverted yellow triangle in 4.2b. If the UAV spends at least one time step in that yellow, it cannot cut the corner.

$$\neg \bigwedge_i slack_{i,n} \quad 0 \leq n \leq N \quad (4.3)$$

Richards and Turnbull[?] proposed a method which prevents corner cutting. In their method, the UAV is considered on the safe side of an edge only if that is true for two consecutive time steps. This is visualized in Figure 4.2. They apply the same constraints again, but this time on the position of the UAV in the last time step:

$$\neg slack_{i,n} \rightarrow \begin{cases} y_{n-1} - v_i & \geq & a_i x_{n-1} + b_i, & \Delta q_{x,i} < 0 \\ y_{n-1} + v_i & \leq & a_i x_{n-1} + b_i, & \Delta q_{x,i} > 0 \\ x_{n-1} + r & \leq & q_{x,i}, & \Delta q_{y,i} < 0, & \Delta q_{x,i} = 0 \\ x_{n-1} - r & \geq & q_{y,i}, & \Delta q_{y,i} > 0, & \Delta q_{x,i} = 0 \end{cases} \quad (4.4)$$

4.2.1 Goal conditions

Forcing the UAV to exactly reach each intermediate goal position is overly restrictive. Because the goal conditions are only checked for each time step, the arrival at the goal position must line up with a time step. If this is not the case, the UAV could be right before the goal position on one time step, and already have passed the goal position by the next time step. The result is that the UAV will slow down near the end of each segment so it can exactly line up with the goal position for that segment. This effect gets worse as the velocity increases.

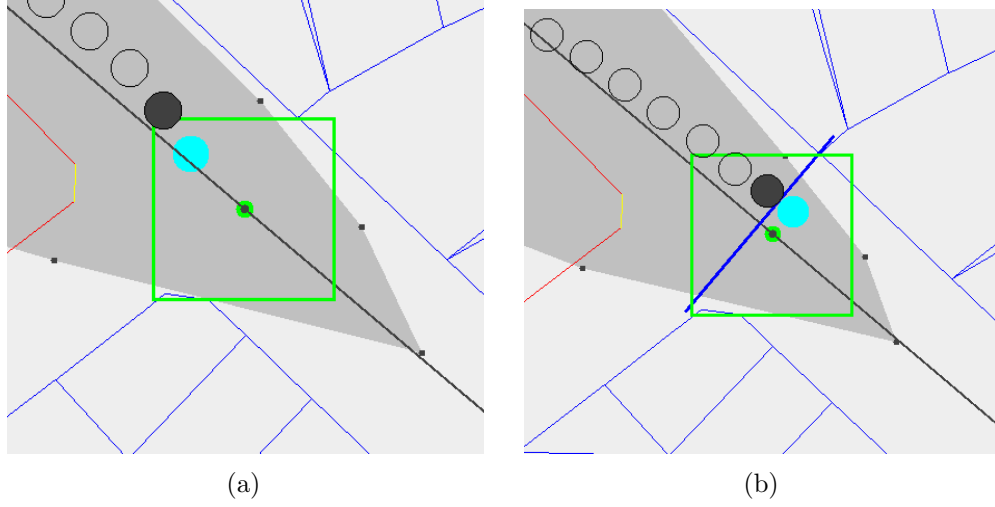


Figure 4.3: 4.3a shows the UAV right before reaching its goal. The blue circle shows the position of the UAV at the segment transition. The goal position is the green dot, while the square around it shows the tolerance region where the goal is considered to be reached. Note how the segment transition happens earlier because of the tolerance region. 4.3b shows the same, only this time a (blue) finish line is added. This time, the UAV needs to cross the finish line so it so the segment transition is roughly as far along the path as planned.

By allowing some difference between the goal position and the position of the UAV, this behavior can be resolved. However, this tolerance on the UAV's position means that the goal condition tends to be satisfied before the UAV has actually reached the goal. This is visible in Figure 4.3a. By adding a finish line perpendicular to the path at the goal position and forcing the UAV to cross this line, this early finish can be counteracted. The tolerance makes the trajectory less restricted, while the finish line ensures that the segment transitions happen at the right time. This can be seen in Figure 4.3b.

4.3 Stability Improvements

4.3.1 Maximum goal velocity

When two corners are close to each other, it may not be possible to expand each corner outwards by the full expansion distance. In that case, the middle between those corners is chosen as the transition between the segments for each corner. This ensures that both corners get a fair share of the space between them. However, it breaks the assumption behind the corner expansion. If the velocity after the first corner is high, due to the reduced approach distance, the UAV may not be able to stop in time for the corner. In this situation, no solution will be found in the second segment. Figure 4.4 shows a situation when this may be necessary.

As a solution for this, the UAV's velocity at the goal of the first segment can be

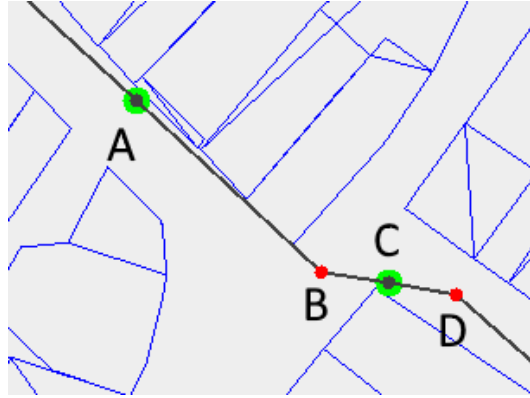


Figure 4.4: A visual demonstration of when a maximum goal velocity is used. Points B and D are individual turn events. The segment for event B starts at A, with $|AB|$ being the desired expansion distance for the segment. However, because D is so close to B, the end of the segment C cannot be placed at the desired expansion distance from B. Instead, C is placed in the middle between B and D, such that $|BC| = |CD|$. The first segment solves the trajectory from A to C past turn event B, the second segment starts as C, past D and onwards. The goal is to ensure that the UAV can still safely stop at D when it starts the second segment at C. This is done by limiting the maximum velocity of the UAV when it reaches the goal C in the first segment.

limited so it can stop in time for the corner in the next segment. The maximum distance at the goal of the segment is v'_{max} , given the actual expansion distance $dist$ in Equation 4.5.

$$v'_{max} = \sqrt{2 * dist * a_{max}} \quad (4.5)$$

4.3.2 Initial Safe Region

The genetic algorithm is relatively simple and makes no attempt to construct the safe region such that the UAV can always stay inside it. This is problematic when the UAV has a long maximum acceleration distance. This problem presents itself in two ways.

The first issue arises at the start of the segment. The maximum goal velocity from section 4.3.1 limits the UAV's velocity, but it does not determine which way the vector is pointed. The maximum goal velocity only ensures safety when the velocity vector is pointed along the path. If the velocity vector is not pointed entirely along the path, the UAV may not be able to stay within the safe region generated by the genetic algorithm. This can be seen in Figure 4.5. The solution to this issue is including the "stop point" in the initial set of points used as the safe region. This stop point is the position where the UAV would come to a halt if it starts decelerates as at the start of the segment. This depends on the initial velocity vector for that segment.

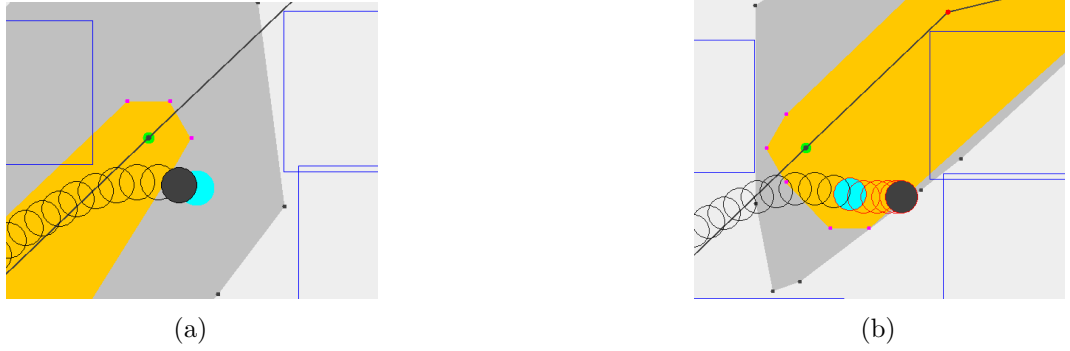


Figure 4.5: An example of how transition between segments can fail. In 4.5a, shows the UAV right before the segment transition which happens at the blue circle. 4.5b shows the orange initial safe region and dark grey expanded safe region of the next segment, after the transition. The next segment fails to solve because the UAV cannot come to a stop within the safe region. The position of the UAV shows where the UAV came to a stop in the previous segment (the safe region of which is the grey region in 4.5a).

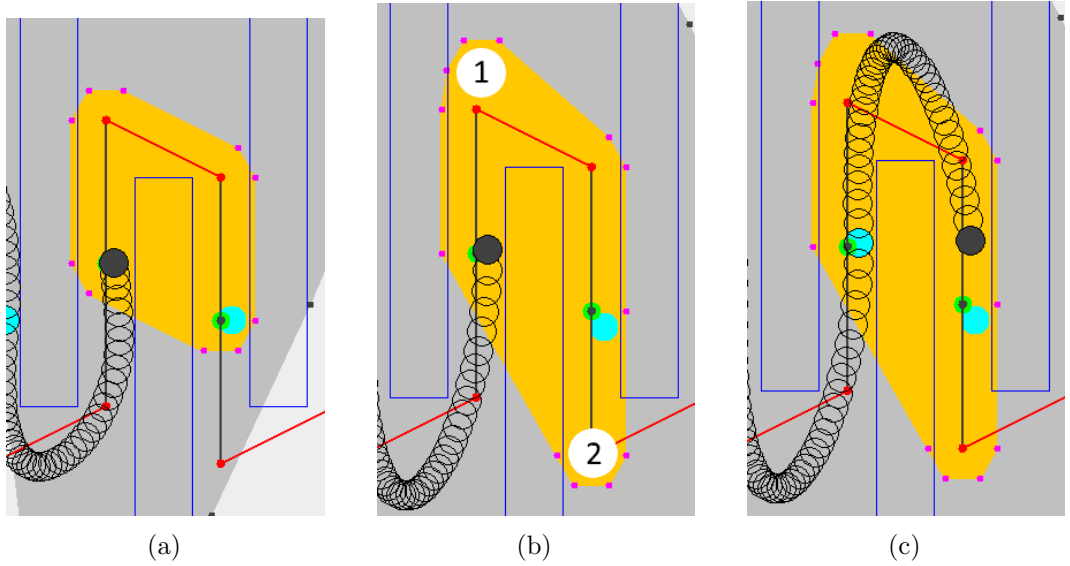


Figure 4.6: 4.6a shows the initial safe region without the extra stop points in orange. 4.6b shows the initial safe region with the extra stop points. The position marked with "1" is the stop point for the initial velocity, while the position marked with "2" is the stop point for the trajectory after the goal has been reached. 4.6c shows how the stop point ensured that the UAV could stop. The UAV leaves the initial safe region because it already has started to turn, however the stop point clearly provided enough space.

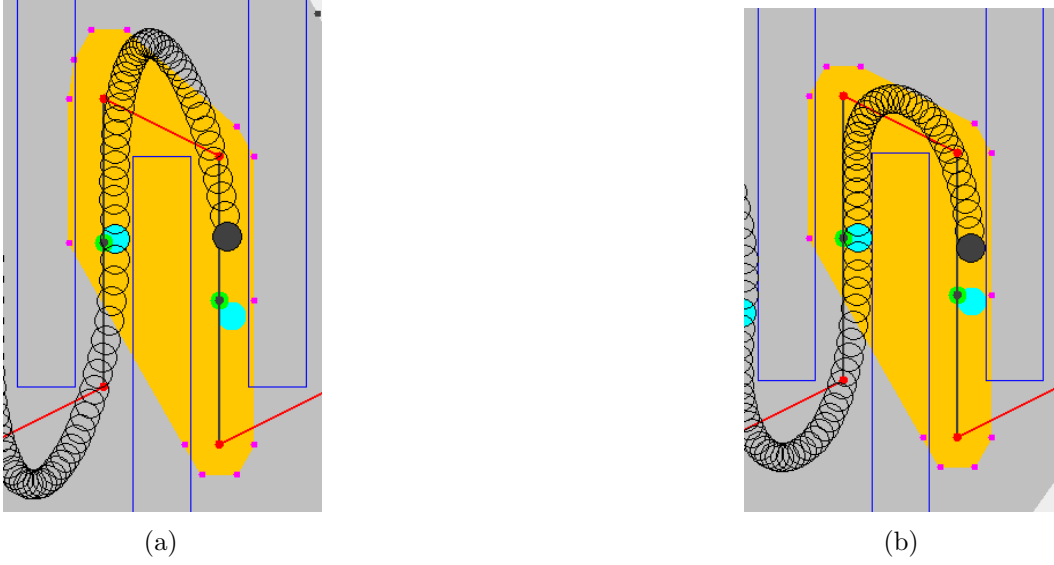


Figure 4.7: 4.7a and 4.7 show the trajectory respectively without and with the maximum goal velocity enabled. In 4.7a, the UAV overshoots the corner which results in a slower trajectory.

The second issue comes into play at the end of a segment. The sub-trajectory for each segment does not end when the goal is reached. It must be calculated for all available time steps. The safe region may be very restrictive just after the UAV has reached its goal. The result is that the UAV has to slow down *before* it reaches its goal to ensure the rest of the trajectory stays within the safe region. This can also be counteracted by including a stop point in the safe region. This time, the velocity vector of the UAV is not known in advance (since the segment has not been solved yet). The velocity vector is assumed to point along the path and the magnitude is either the maximum goal velocity or maximum velocity, depending on whether the maximum goal velocity is defined.

Figure 4.6 shows the result when both of these stop points are included. In the example, the maximum goal velocity has been ignored to exaggerate the effect. However, the extra stop points should always be used together with the maximum goal velocity. The stop points allow the UAV to make the transition between segments at higher velocities, but that also means they can overshoot in turns. This is demonstrated in Figure 4.7.

4.4 Overlapping segment transitions

The initial safe region extensions (section 4.3.2), more tolerant goal condition (section 4.2.1) and the maximum goal velocity (section 4.3.1) often improve the quality of the trajectory. However, they do not deal with all cases in which a bad segment transition happens, as demonstrated in Figure 4.8. The trajectory up to the goal of

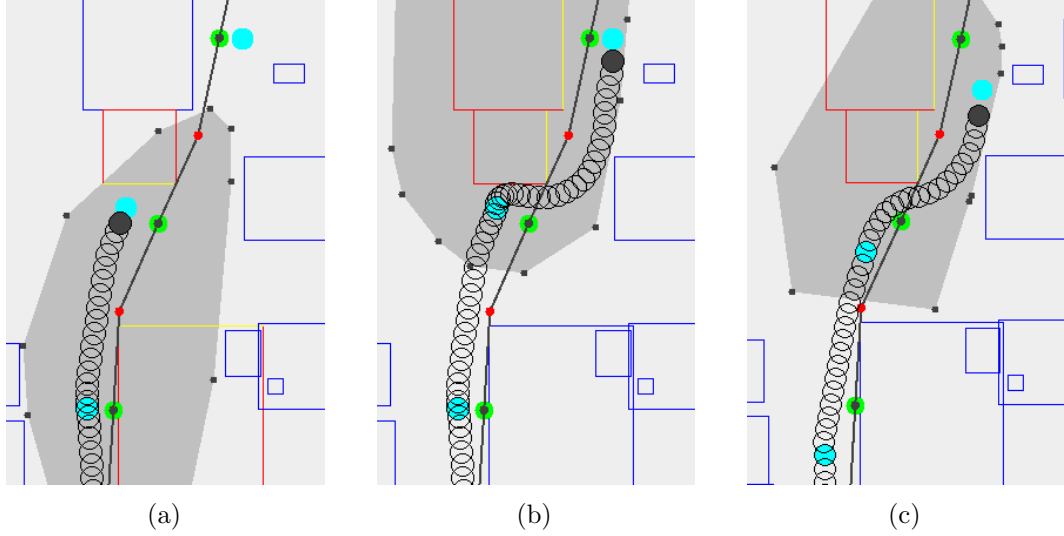


Figure 4.8: 4.8a shows the optimal approach to the goal of the previous segment. However, as seen in 4.8b, this is a very bad start state for the next segment. By starting the next segment 5 time steps earlier in 4.8c, this bad approach can be partially mitigated.

the first segment is optimal (Figure 4.8a), but provides a really bad start for the next segment (Figure 4.8b).

This can be counteracted by starting the next segment earlier than usual. Instead of starting at the time step where the goal in the previous segment is reached, the next segment start several time steps earlier. This ensures the the previous segment still attempts to reach its goal as fast as possible, but also allows the next segment to correct for suboptimal transitions earlier. This can be seen in Figure 4.8c.

4.5 Graphical Visualization Tool

Using MILP to solve the trajectory planning problem makes my algorithm flexible. Different constraints can be added and removed without having to change complex algorithm. The solver takes those changes into account and still finds a solution. This declarative approach makes it much easier to experiment with different variants of the problem, however it does also have downsides. One of those downsides is that it becomes harder to understand why the solution to the problem is what it is. Especially since MILP solvers don't provide a lot of useful insight during execution. This problem is made worse by the fact that the trajectory planning problem is an optimization problem. We're not just interested in having any solution, but instead we want a good or possibly even the best solution.

These factors make the MILP solvers a "black box". This is especially problematic when they fail to find a solution. Most solvers will inform you which constraint caused the failure, but that constraint is not necessarily the one that is incorrect.

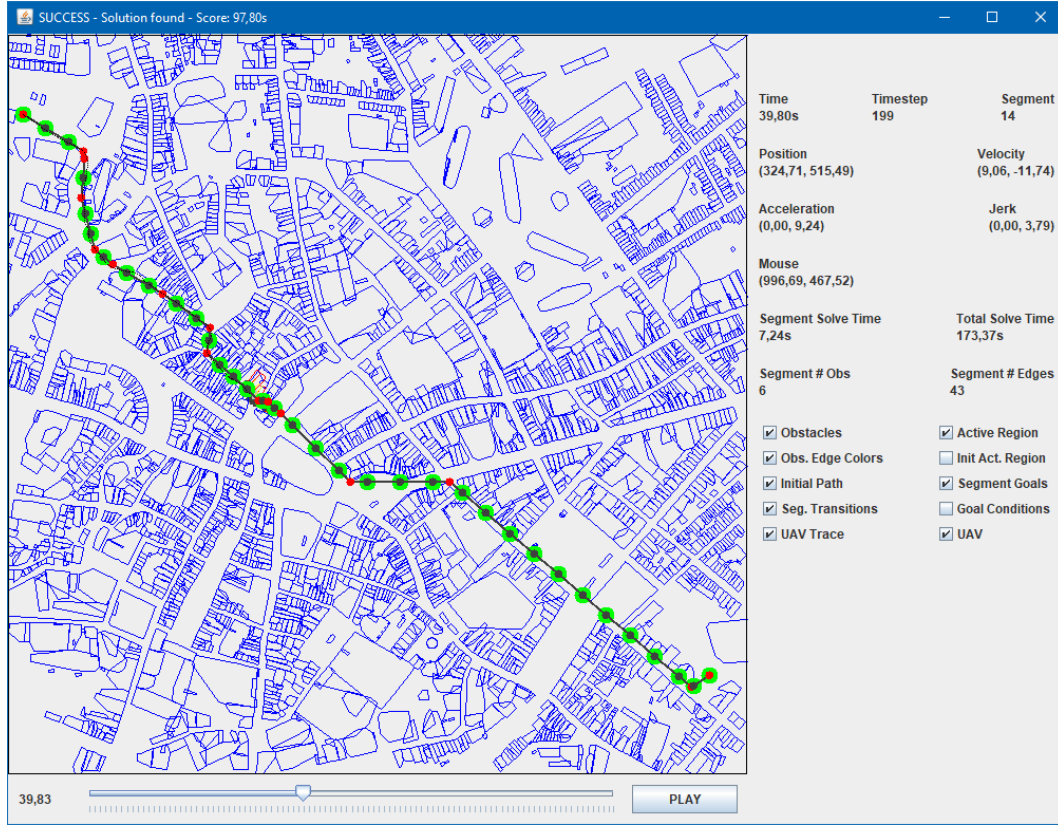


Figure 4.9: An overview of the visualization tool that shows the results of the algorithm.

Another constraint may have made the problem impossible to solve, but the solver will only fail by the time it leads to a contradiction.

Another problem is figuring out if all constraints are actually modeled properly. A badly modeled constraint may have no effect at all, or a different effect than intended. Gaining a deep understanding of what is happening is an issue as more and more constraints are added and the interactions between them increase.

For this reason, I spent a significant amount of time building a visualization tool which displays not only the solution, but also the constraints of the MILP problem and other debugging information. This proved to be a critical part of the development cycle of the algorithm. Figure 4.9 shows this tool. At first glance, the tool may look familiar. It has been used to create every example shown in this thesis.

4.5.1 Interface Elements

The graphical interface is divided into three parts.

World view The first and most prominent part is the visualization on the left. This shows a view of the world with a variety of information overlaid on top of it. The view can be translated by holding down the left mouse button and dragging around. Scrolling zooms in and out on the view.

Timeline The second element is the timeline on the bottom. By dragging the slider, the user can change the time step being visualized. There is also a play/pause button which can be used to animate the visualization. The animation runs in realtime according to the progress of time of the trajectory. The animations help spot more subtle changes in acceleration which are not immediately clear from the still view.

Data Panel The last element is the panel on the right. This panel contains more detailed information about the current time step being visualized. This information includes:

- The current time in the trajectory
- The current time step number
- The current segment number
- The position, velocity, acceleration and jerk (derivative of acceleration) at the current time step
- The world coordinates at the position of the mouse
- The solve time for the current segment
- The total execution time of the entire algorithm
- The amount of obstacles and edges being modeled in the current segment

On top of that information, there are also visibility toggles for the various elements of the visualization.

4.5.2 World View Elements

Obstacles The obstacles are the most common element in the visualization. Obstacles are visualized as blue polygons. See Figure 4.10.

Initial path The initial path is the result of the Theta* algorithm. It is shown as black lines. The turn events on this path are red. When multiple nodes on the path belong to the same turn event, the lines connecting them are also red. See Figure 4.10.

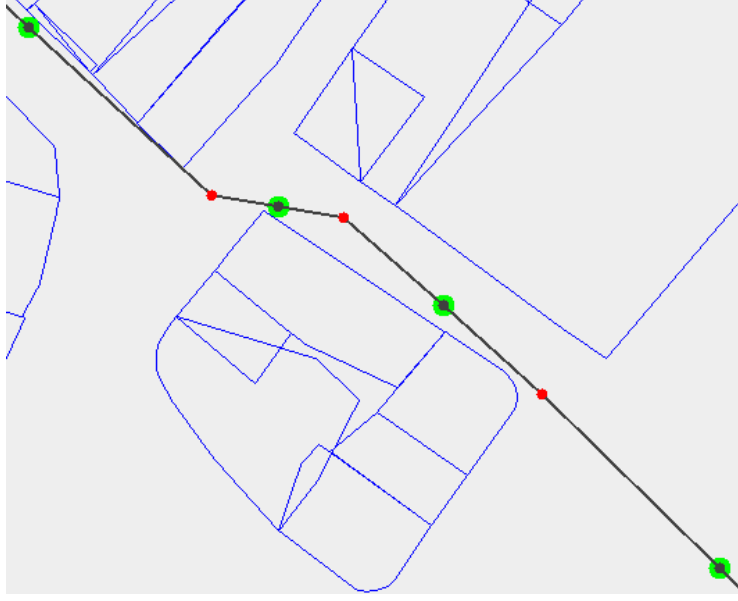


Figure 4.10: The obstacles are blue, initial path is black with turn events being red. The green circles are the segment goals.

Scenario goals The scenario goals are visualized as the green circles on the initial path. These goals mark both the end of a segment and the start of the next segment. See Figure 4.10.

Safe region The safe region for the current segment, the result from the genetic algorithm, is shown as a dark grey polygon. The UAV must stay within this polygon at all times. See Figure 4.11.

Obstacle Edge Colors The obstacles within the safe region are modeled in the MILP problem. The color of the edges of these obstacles displays whether or not the constraint is active for that edge at the current time step. If the color is yellow, the UAV is on the safe side of the obstacle. Otherwise, the color is red. See Figure 4.11.

Segment Transitions The segment transitions do not always happen right at the goal positions of the segments. The light blue circle shows the position of the UAV at the time of the actual segment transition. See Figure 4.11.

Initial Safe Region Before the genetic algorithm is executed, an initial safe region is constructed which ensures the UAV can reach its goal in the current segment. This initial safe region is shown in orange. The (expanded) safe region from the genetic algorithm must completely contain this initial region. See Figure 4.12.

Goal Conditions The UAV does not have to reach its goal exactly. The green square around the segment goal shows the tolerance region where the UAV is close enough

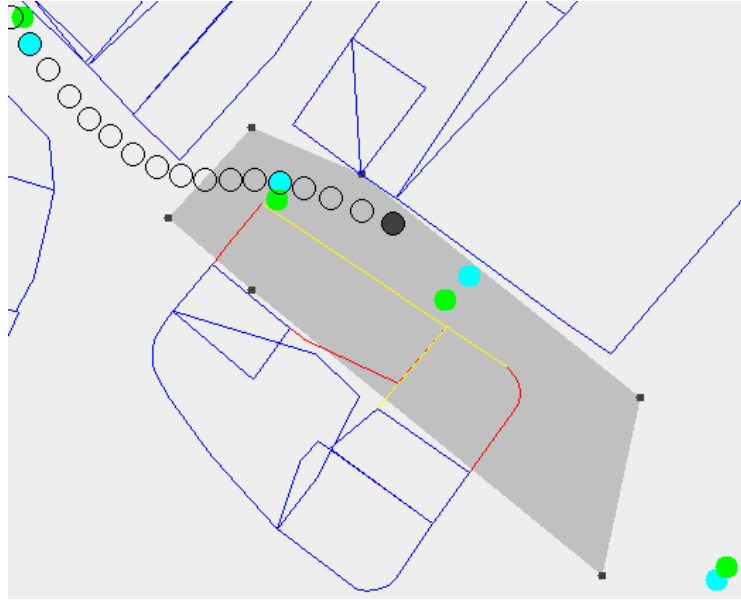


Figure 4.11: The safe region is dark grey and the segment transitions are light blue. The edges of the obstacles inside the safe region are yellow or red to signify whether or not the UAV is on the safe size of that edge.

to its goal. The blue line shows the finish line which the UAV must cross as well. See Figure 4.12.



Figure 4.12: The initial safe region is shown in orange. To reach its goal, the UAV must be inside the green square and have crossed the blue finish line.

Experiments and Results

5.1 Scenarios

Several different scenarios are used to test the algorithm. Each scenario takes place in a world with a certain distribution of obstacles, has a start and goal position, and a UAV with certain characteristics.

There are three categories of scenarios, which will be discussed in section 5.1.1 to 5.1.3. All scenarios are tested in a general performance test (section 5.2) to get an overview of the performance of the algorithm with the default parameters. This test determines whether or not the algorithm scales to large and complex environments. In the other tests, only one scenario of each category has been used. Section 5.3 tests the performance of the algorithm as the characteristics of the UAV change. Section 5.4 looks at the stability of the algorithm. These tests should provide further insight on the limitations of the algorithm.

Sections 5.5 to 5.9 look at the effects of different parameters on both the performance of the algorithm and the quality of the trajectory. Sensible default parameters have been chosen. However, changing these parameters provides deeper insights in the characteristics of the algorithm.

All tests were executed on an Intel Core i5-4690k running at 4.4GHz with 16GB of 1600MHz DDR3 memory. The reported times are averages of 5 runs, unless stated otherwise. The machine runs on Windows 10 using version 12.6 of IBM CPLEX. Table 5.1 show the default parameters as used in all tests.

grid size	$2m$	turn tolerance	2
approach multiplier	2	population size	10
# generations	25	max. nudge distance	$5m$
min. # vertices	4	max. # vertices	12
P(add vertex)	0.1	P(remove vertex)	0.1
max nudge attempts	15	T_{max}	$5s$
time step size	$0.2s$	position tolerance	3
CPLEX max solve time	$120s$	CPLEX max delta	1
time limit multiplier	1.5	max segment time	$3s$
linear approx vertices	12		

Figure 5.1: The parameters used for testing

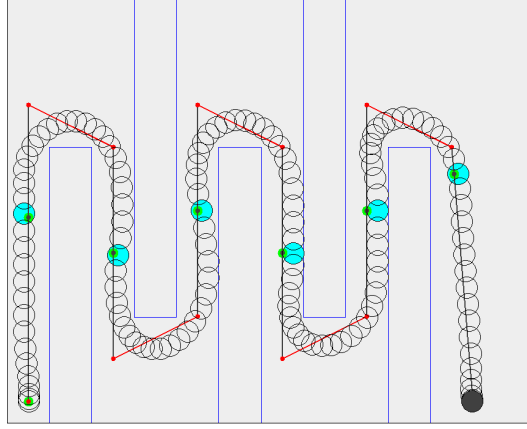
5.1.1 Synthetic Scenarios

The synthetic scenarios have small, handmade worlds. They have few obstacles, but the obstacles are laid out in a way that makes them challenging to solve. There are two "Up/Down" scenarios, small (Figure 5.2a) and large (Figure 5.2b), in which the UAV has to move in a zig-zag pattern to reach its goal. The difference between those scenarios is the amount of obstacles, which also changes the amount of zig-zags required. These scenarios are built to see how the algorithm handles sharp turns. There is also a spiral scenario in which the UAV must go in an outwards spiral (Figure 5.2c).

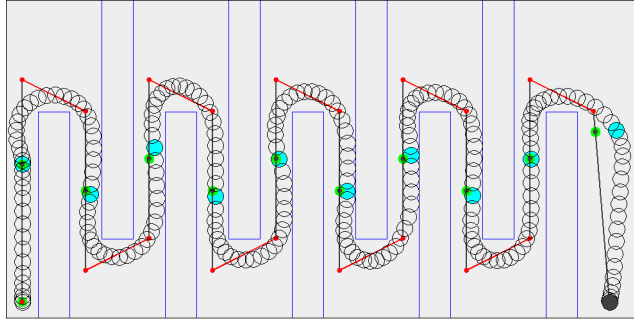
The large Up/Down scenario represents this category in the tests. Table 5.1 shows the properties of the UAV.

$v_{max} \text{ (ms}^{-1}\text{)}$	$a_{max} \text{ (ms}^{-2}\text{)}$	radius (m)
3	4	0.5

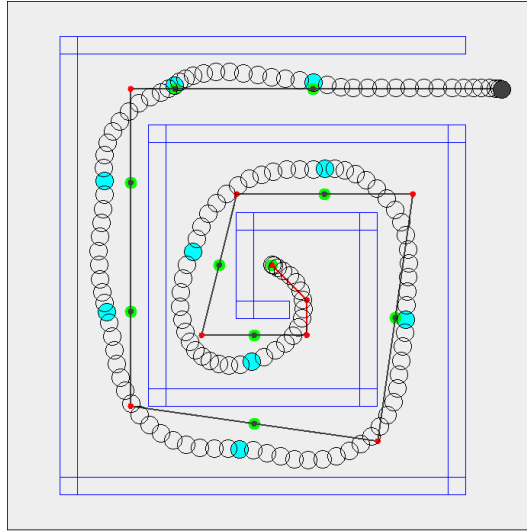
Table 5.1: The UAV properties for the synthetic scenarios



(a)



(b)



(c)

Figure 5.2: The synthetic scenarios

5.1.2 San Francisco Scenarios

The San Francisco scenarios contain a world which is based on a map of San Francisco. There are 2 small San Francisco scenarios (Figure 5.4a and 5.4b), which both share the same 1km by 1km area of San Francisco but have different start and goal locations. There is also a larger San Francisco scenario which takes places on a 3km by 3km world (Figure 5.4c).

All obstacles in the San Francisco dataset are grid-aligned rectangles, laid out in typical city blocks. Because of this, density of obstacles is predictable. These scenarios showcase that the algorithm can scale to realistic scenarios with much more obstacles than is typically possible with a MILP approach.

The first small San Francisco scenario is used to represent this category in the tests. Table 5.2 shows the properties of the UAV and Figure 5.5 shows a zoomed-in view of the first small scenario.

$v_{max} (ms^{-1})$	$a_{max} (ms^{-2})$	radius (m)
10	15	2.5

Table 5.2: The UAV properties for the San Francisco scenarios

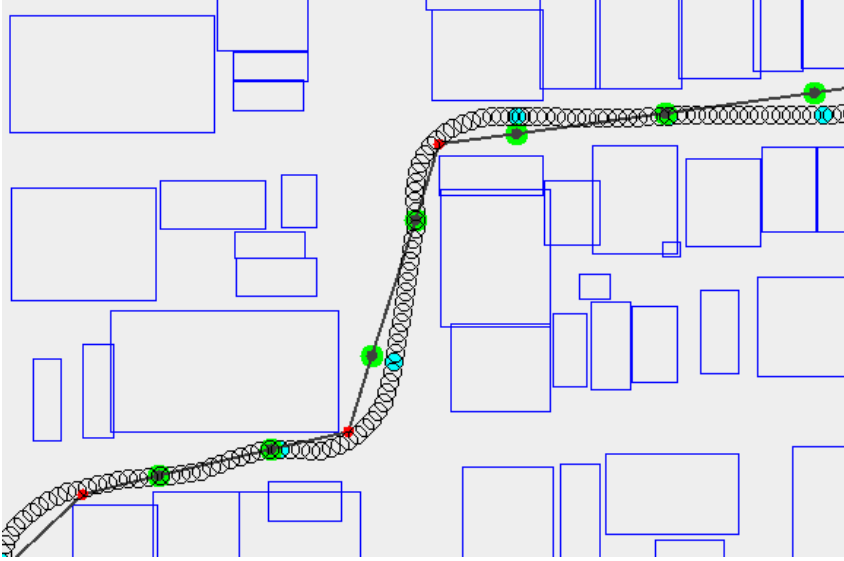


Figure 5.3: A zoomed-in view of the first small the San Francisco scenario

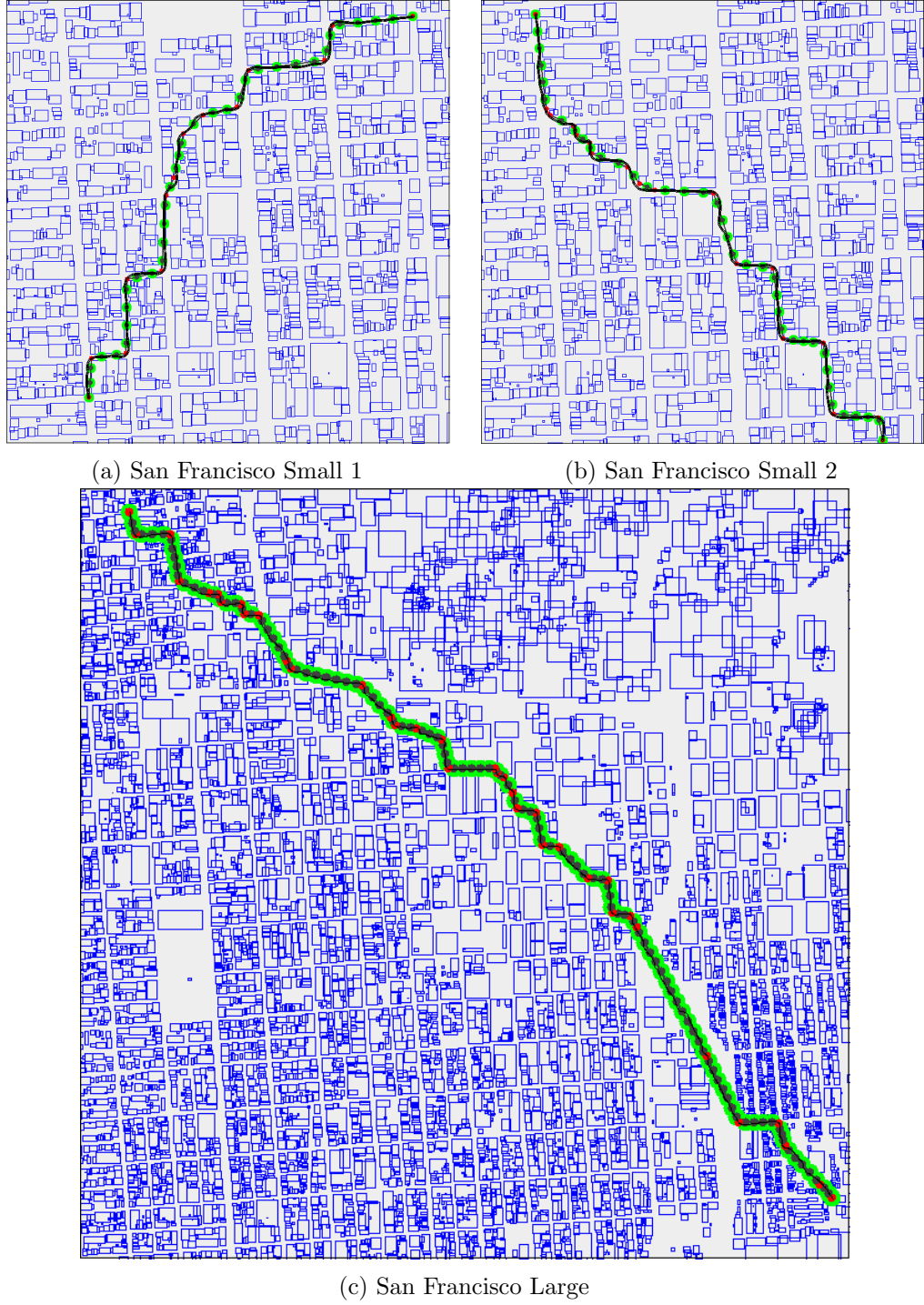


Figure 5.4: The San Francisco scenarios

5.1.3 Leuven Scenario

The Leuven scenarios contain a world based on a map of the city of Leuven. This is an old city with a very irregular layout. The dataset, provided by the local government¹, also contains full polygons instead of the grid-aligned rectangles of the San Francisco dataset. While most buildings in the city are low enough so a UAV could fly over, it presents a very difficult test case for the path planning algorithm. The density of obstacles varies greatly and is much higher than in the San Francisco dataset across the board.

The first small Leuven scenario is used to represent this category in the tests. Table 5.3 shows the properties of the UAV and Figure ?? shows a zoomed-in view of the first small scenario.

$v_{max} \text{ (ms}^{-1}\text{)}$	$a_{max} \text{ (ms}^{-2}\text{)}$	radius (m)
10	15	1

Table 5.3: The UAV properties for the Leuven scenarios



Figure 5.5: A zoomed-in view of the first small the Leuven scenario

¹<https://overheid.vlaanderen.be/producten-diensten/basiskaart-vlaanderen-grb>

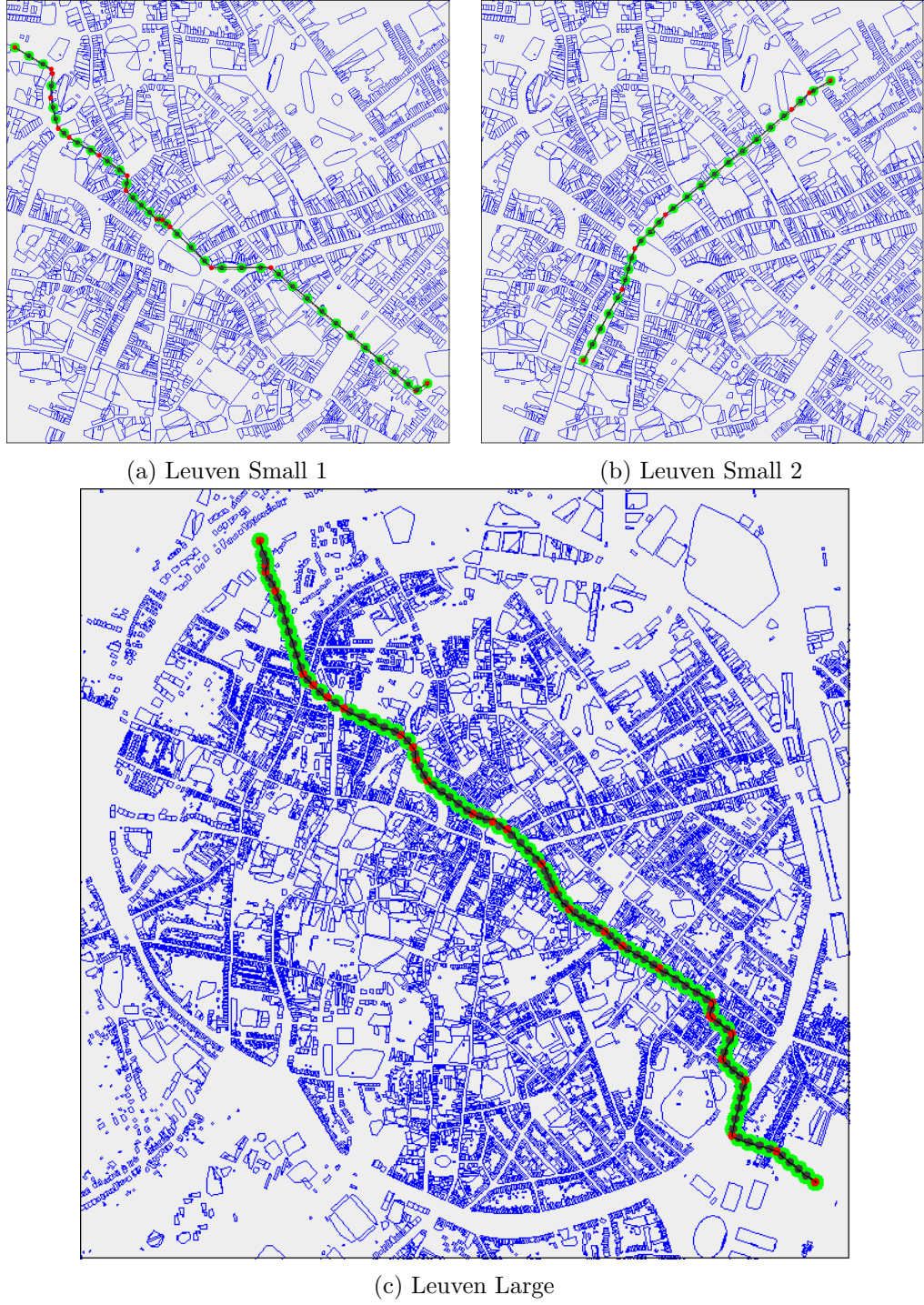


Figure 5.6: The Leuven scenarios

Scenario name	# obstacles	world size	path length (m)	# segments
Up/Down Small	5	25m x 20m	88	7
Up/Down Large	9	40m x 20m	146	11
Spiral	11	30m x 30m	96	10
SF Small 1	684	1km x 1km	1392	34
SF Small 2	684	1km x 1km	1490	38
SF Large	6580	3km x 3km	4325	107
Leuven Small 1	3079	1km x 1km	1312	34
Leuven Small 2	3079	1km x 1km	864	22
Leuven Large	18876	3km x 3km	3041	78

Table 5.4: Some information about the scenarios tested.

Scenario name	Theta* (s)	GA (s)	MILP (s)	total (s)	score (s)
Up/Down Small	0.00	0.33	10.48	10.97	27.24
Up/Down Large	0.00	0.65	17.95	18.87	44.76
Spiral	0.01	1.06	7.17	8.46	28.72
SF Small 1	1.37	7.68	32.81	42.43	106.20
SF Small 2	1.82	7.98	36.81	47.32	114.36
SF Large	15.88	15.41	75.44	108.28	325.10
Leuven Small 1	1.51	23.49	135.86	161.85	97.44
Leuven Small 2	0.53	14.00	62.03	76.99	65.52
Leuven Large	14.65	67.55	460.46	544.73	227.27

Table 5.5: A breakdown of the execution time for each scenario, as well as the score of the trajectory.

5.2 General Performance

In this test, the general performance of the different parts of the algorithm are tested. Every scenario is tested with the default parameters. Table 5.4 shows some detailed information about the scenarios, including the length of the Theta* path and the amount of segments problem is divided into. Table 5.5 shows the execution parts for the most computationally expensive parts of the algorithm (the Theta* path, genetic algorithm and MILP solver), as well as the total time required. It also shows the score of the resulting trajectories. This score is in seconds and is the amount of time that the UAV needs to reach the goal position when following the trajectory.

5.2.1 Interpretation

With the default settings, the algorithm is capable of solving all scenarios within a reasonable amount of time. In every case, solving the MILP problem takes the majority of the time.

The amount of segments differs between these scenarios. Table 5.6 expresses the results relative to the amount of segments, as well as the path length per segment.



(a) The large San Francisco scenario has a region with very sparse obstacles.

(b) The large Leuven scenario passes through several regions with very dense obstacles

Figure 5.7

Scenario name	path length(m)	Theta* (s)	GA (s)	MILP (s)	total (s)
Up/Down Small	12.57	0.00	0.05	1.50	1.57
Up/Down Large	13.27	0.00	0.06	1.63	1.72
Spiral	9.60	0.00	0.11	0.72	0.85
SF Small 1	40.94	0.04	0.23	0.97	1.25
SF Small 2	39.21	0.05	0.21	0.97	1.25
SF Large	40.42	0.15	0.14	0.71	1.01
Leuven Small 1	38.59	0.04	0.69	4.00	4.76
Leuven Small 2	39.27	0.02	0.64	2.82	3.50
Leuven Large	38.99	0.19	0.87	5.9	6.98

Table 5.6: A breakdown of the execution time per segment

A first observation is that the path length per segment is very similar for all San Francisco and Leuven segment. The UAV has the same maximum velocity and acceleration in those scenarios. Even though the density and layout of the obstacles is very different, the amount of segments scales linearly with the path length as long as the UAV properties remain the same.

Another observation is that the relative time needed to calculate the Theta* path increases as the path length increases. This is not surprising since Theta*, like A*, has an exponential worst-case complexity. This means that the scalability of Theta* puts an upper limit on the scalability of the entire algorithm.

The next observation is the genetic algorithm (GA) execution time and MILP solve times are very similar within categories. For the synthetic category, the Up/Down scenarios are virtually identical in both measures. The spiral scenario is hard to compare since it is very different.

For the San Francisco scenarios, the two small scenarios have very similar GA and MILP execution times, but the larger scenario comes in lower. The two small Leuven scenarios are also similar in GA execution time, although the first scenario has a higher MILP solve time. The large Leuven scenario has higher execution times for both the GA and MILP solver.

These variations can be explained by differences in densities between the scenarios. In the large San Francisco scenario, the trajectory crosses a region with very sparse buildings (Figure 5.7a). The sections in the regions are easier to solve than in the smaller scenarios. The opposite happens in the large Leuven scenario, which passes through several regions with very dense obstacles (Figure 5.7b). These account for the significant increase in execution time for both the genetic algorithm as the MILP solver.

5.3 Agility of the UAV

The properties of the segments strongly rely on the agility of the UAV. The size of the segments is determined by the maximum acceleration distance of the UAV.

This experiment tests the relation between the maximum velocity and the maximum acceleration of the UAV. This test was executed on the standard set of scenarios: the large Up/Down scenario, the small San Francisco scenario and the small Leuven scenario. For each scenario I tested nine configurations of the vehicle: Every combination between three different maximum velocities and three different maximum accelerations. Table 5.7 shows the different UAV properties for the Up/Down scenario, Table 5.8 shows the same properties for the San Francisco and Leuven Scenarios. Table 5.9, 5.10 and 5.11 shows the results for respectively the Up/Down, San Francisco and Leuven scenarios. Figure 5.8, 5.9 and 5.10 show the same data, but fix either the acceleration or velocity and vary the other property.

	Low	Med	High
Velocity (ms^{-1})	2	4	8
Acceleration (ms^{-2})	1	3	6

Table 5.7: The different maximum velocity and acceleration values for the vehicle for the Up/Down scenario.

	Low	Med	High
Velocity (ms^{-1})	5	15	30
Acceleration (ms^{-2})	3	10	20

Table 5.8: The different maximum velocity and acceleration values for the vehicle for the San Francisco and Leuven scenarios.

solve time (s)	Low vel	Med vel	High vel
Low acc	26.08	91.98	100.28
Med acc	9.93	16.93	15.17
High acc	7.23	6.39	4.85

Table 5.9: Up/Down

solve time (s)	Low vel	Med vel	High vel
Low acc	57.3	-	-
Med acc	22.78	31.85	483.17
High acc	19.53	13.75	39.64

Table 5.10: San Francisco

solve time (s)	Low vel	Med vel	High vel
Low acc	127.62	-	-
Med acc	64.16	118.86	-
High acc	60.83	53.8	-

Table 5.11: Leuven

5.3.1 Interpretation

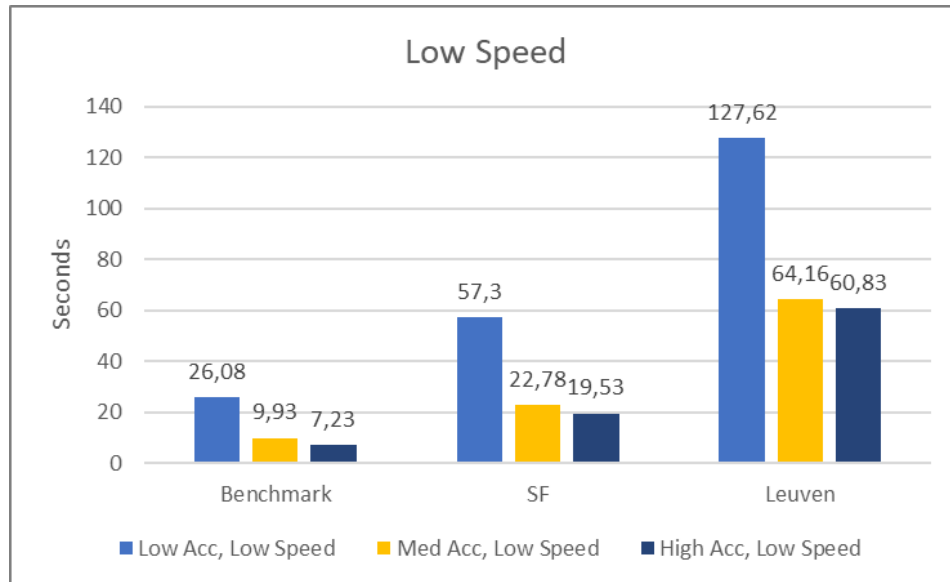
Several of the combinations failed to complete because the segments could not be solved within 120 seconds each. The general trend is that a higher maximum acceleration and a lower maximum velocity decrease the solve time. This is as expected, as both of those make the maximum acceleration distance smaller. A larger maximum acceleration distance leads to larger segments with more obstacles in them, which have a negative effect on the performance.

When the acceleration is high, varying the velocity has an unexpected effect. When going from a low to medium maximum velocity, the solve time actually decreases for all scenarios. I do not have an explanation for why this happens.

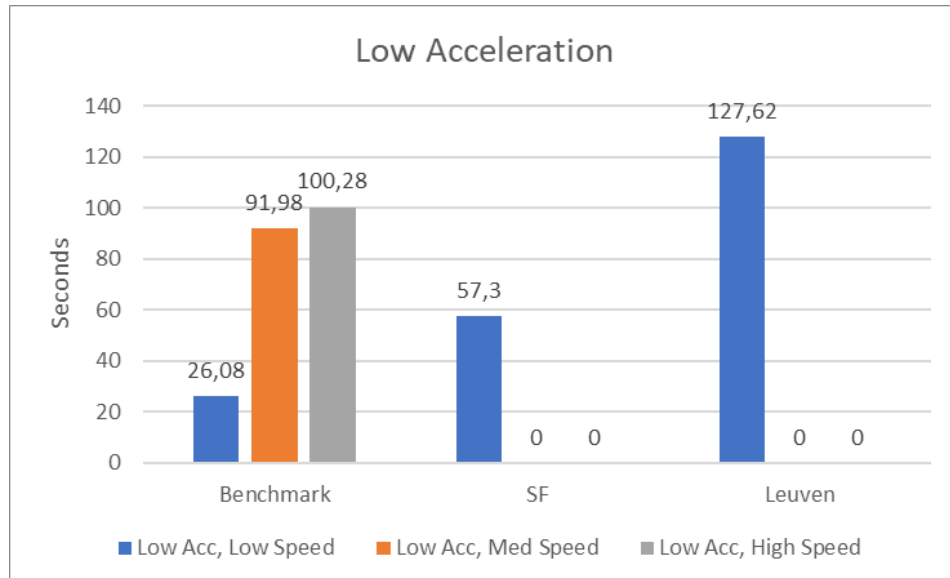
Another slightly unexpected result is that the combination of a high maximum acceleration and high maximum velocity fails for the Leuven scenario. This is not a particularly difficult combination for the other scenarios, so the failure is unexpected.

The default UAV properties seem to be right on the limit for the Leuven scenario. If the UAV is a bit less agile, the algorithm fails to find a solution. This can also be flipped on its head: the Leuven scenario is on the edge of what can be solved. The density of obstacles in the Leuven scenario is at the limit of what can be handled using the default parameters.

5. EXPERIMENTS AND RESULTS

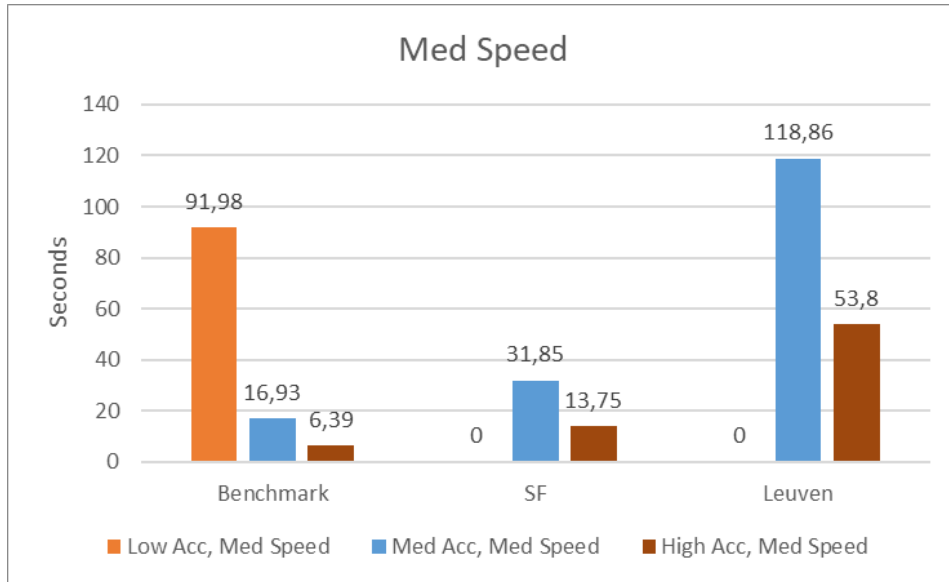


(a) The effects of a varying maximum acceleration and a low maximum velocity.

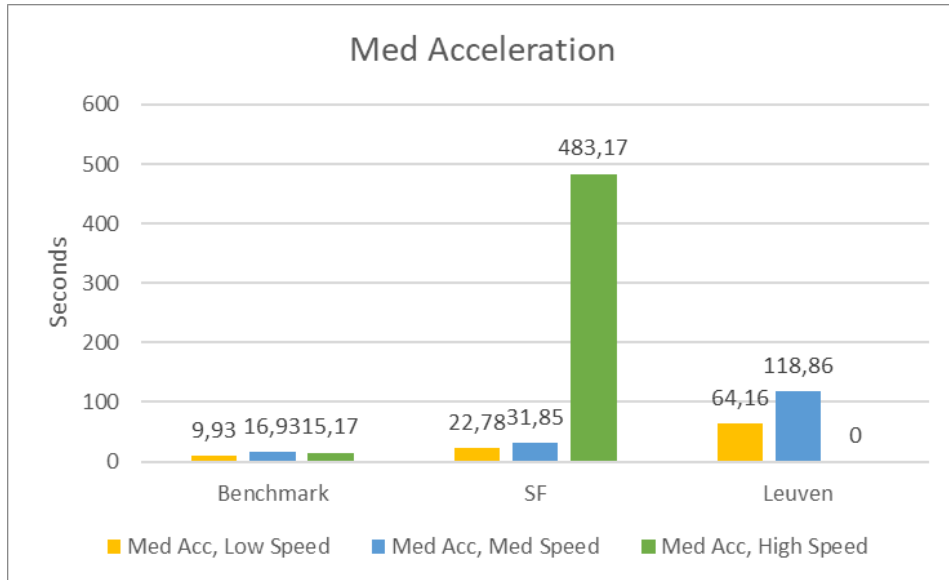


(b) The effects of a varying maximum velocity and a low maximum acceleration.

Figure 5.8



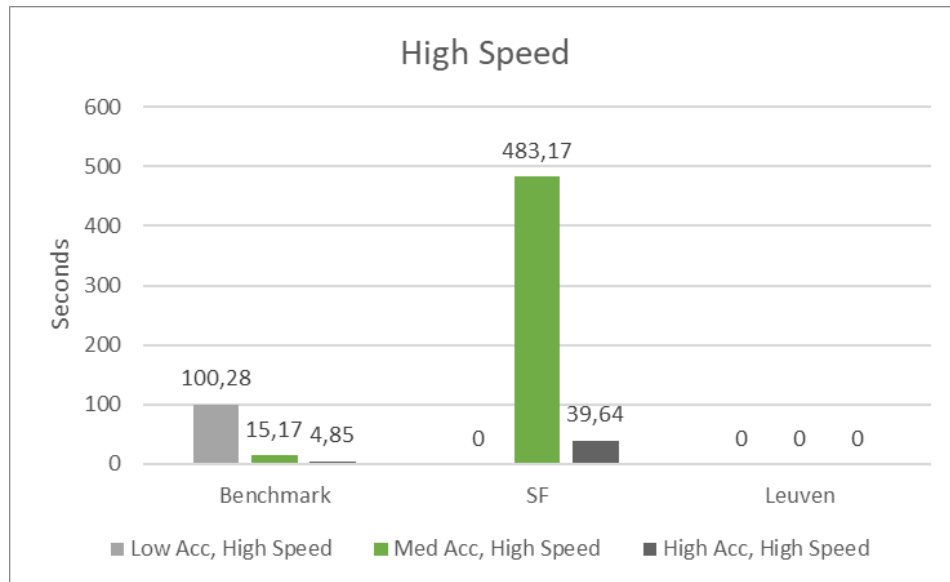
(a) The effects of a varying maximum acceleration and a medium maximum velocity.



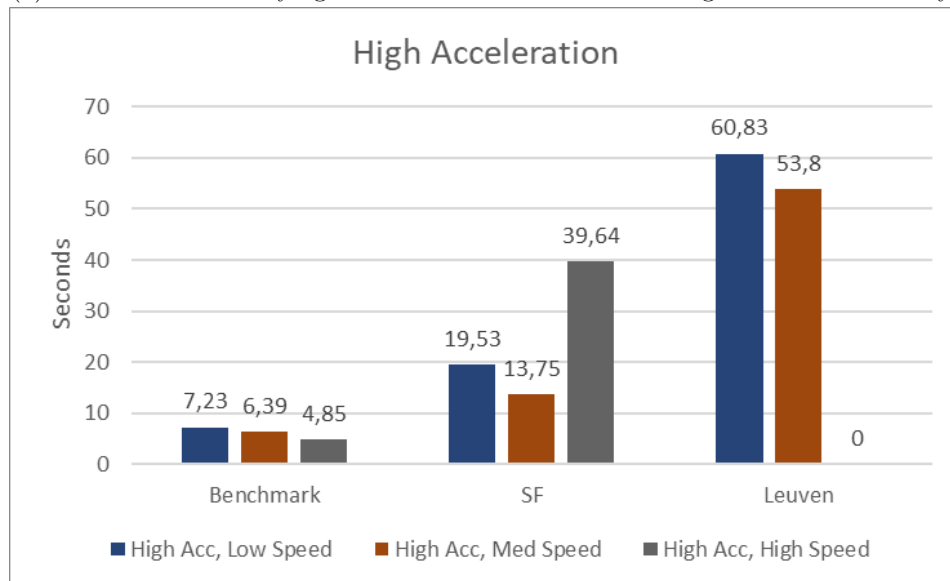
(b) The effects of a varying maximum velocity and a medium maximum acceleration.

Figure 5.9

5. EXPERIMENTS AND RESULTS



(a) The effects of a varying maximum acceleration and a high maximum velocity.



(b) The effects of a varying maximum velocity and a high maximum acceleration.

Figure 5.10

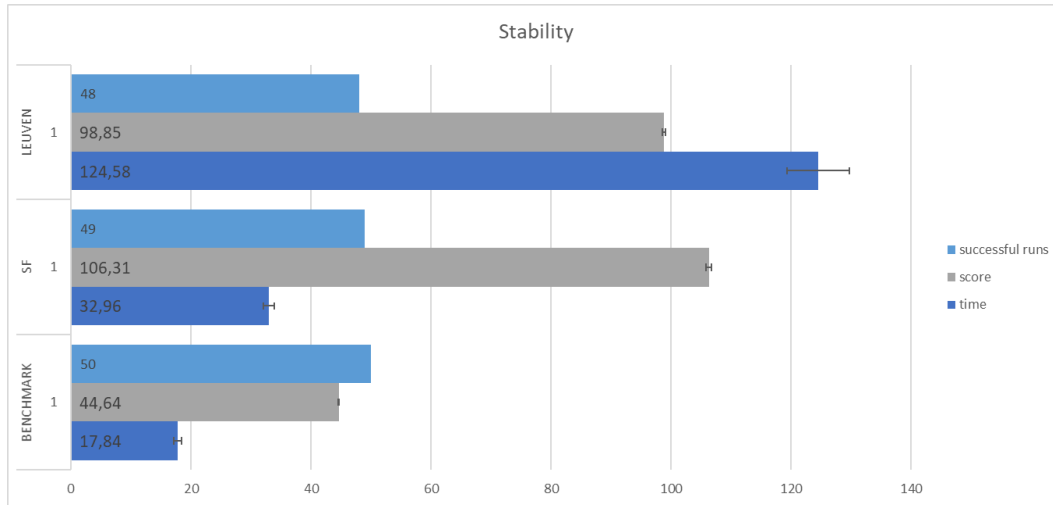


Figure 5.11: stability data

5.4 Stability

Stability is an important property of an algorithm. When the same problem is solved several times, the algorithm should not occasionally fail to solve the problem or require a wildly different amount of time to solve that problem.

This experiment aims to measure the stability of the algorithm. Each of the testing scenarios is executed 50 times, instead of 5 like in the other tests. Figure 5.11 shows the results of this test. The error bars show sample standard deviation.

5.4.1 Interpretation

Even though the each sub-problem should ensure that the next segment can be solved, occasionally this was not the case as demonstrated in Figure 5.12. It seems like a collision is inevitable, but that is actually not the case as demonstrated in 5.13. I believe this may be a bug in how the algorithm transitions between segments. I could not properly figure out what cases this bug in time.

However, the algorithm does find a good trajectory in nearly all cases. When it does succeed, the variation in trajectory score is minimal. The solve time variation is also low, although it is a significantly higher for the Leuven scenario than for the others.

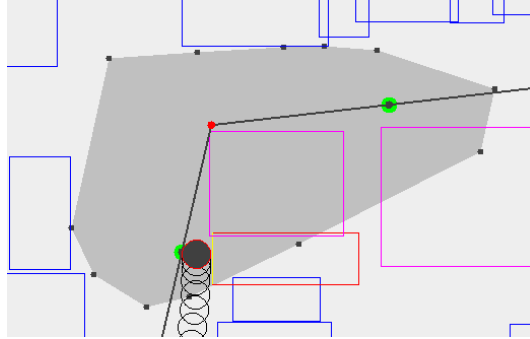
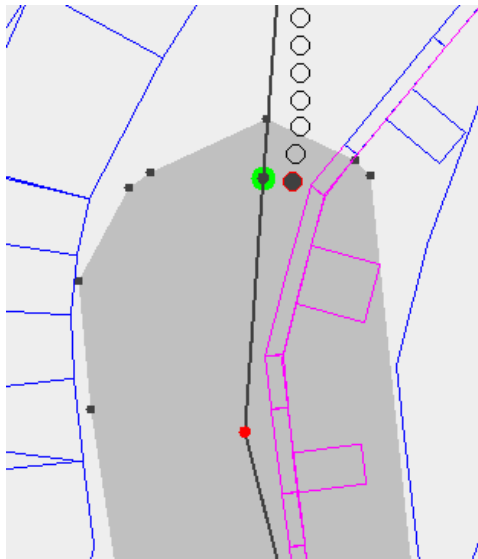
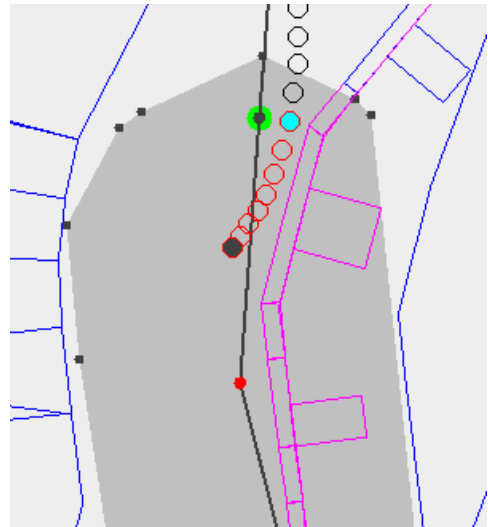


Figure 5.12: A case where the transition between segments fails



(a) This segment starts and fails with what seems like an inevitable collision...



(b) ... However, this shows the trajectory in the previous segment after the goal in that segment has been reached in red. Clearly a collision is not inevitable.

Figure 5.13

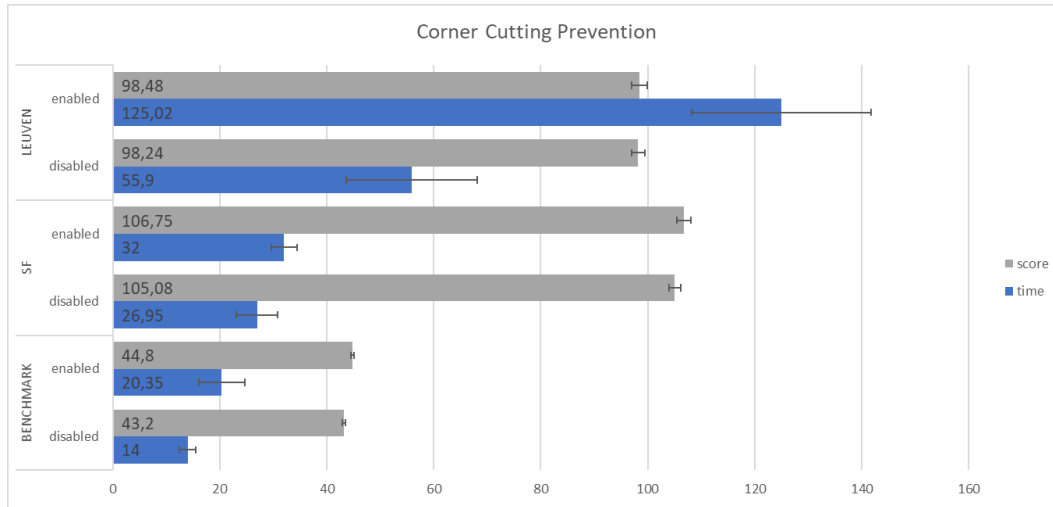


Figure 5.14: The error bars show the 95% confidence interval.

5.5 Cornercutting

A trajectory that allows corner cutting cannot be considered safe. However, additional constraints are required to prevent this from happening. This experiment attempts to measure the impact of the corner cutting prevention. The scenarios are solved with the corner cutting mitigation from section 4.2 both enabled and disabled. Figure 5.14 shows the results.

5.5.1 Interpretation

As expected, enabling the corner cutting prevention has a negative impact on performance. This effect is limited for the Up/Down and San Francisco scenarios. For the Leuven Scenario, the solve time more than doubles. This is likely due to the higher obstacle density and complexity.

5. EXPERIMENTS AND RESULTS

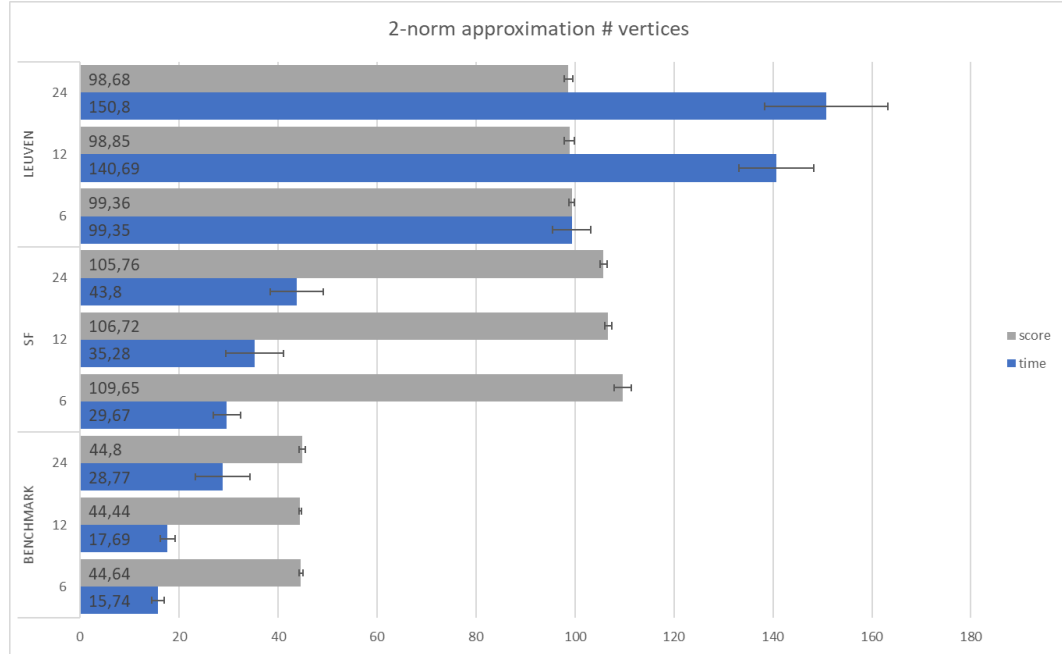


Figure 5.15: linear approx data

5.6 Linear approximation

The velocity and acceleration of the UAV are limited to some finite value. Because both of those quantities are vectors, that maximum can only be approximated with linear constraints. More constraints are needed to model this more accurately which can allow for faster solutions. However, more constraints also have a performance cost. This experiment analyses the trade-off that needs to be made. The amount of vertices used for the linear approximation is tested with values of 6, 12 and 24.

5.6.1 Interpretation

In all cases, increasing the amount of vertices used to approximate the 2-norm also increases the solve time. The effect on trajectory score seems to be minimal for the Up/Down and Leuven trajectory. However, for the San Francisco trajectory there is a noticeable improvement with the better approximation.

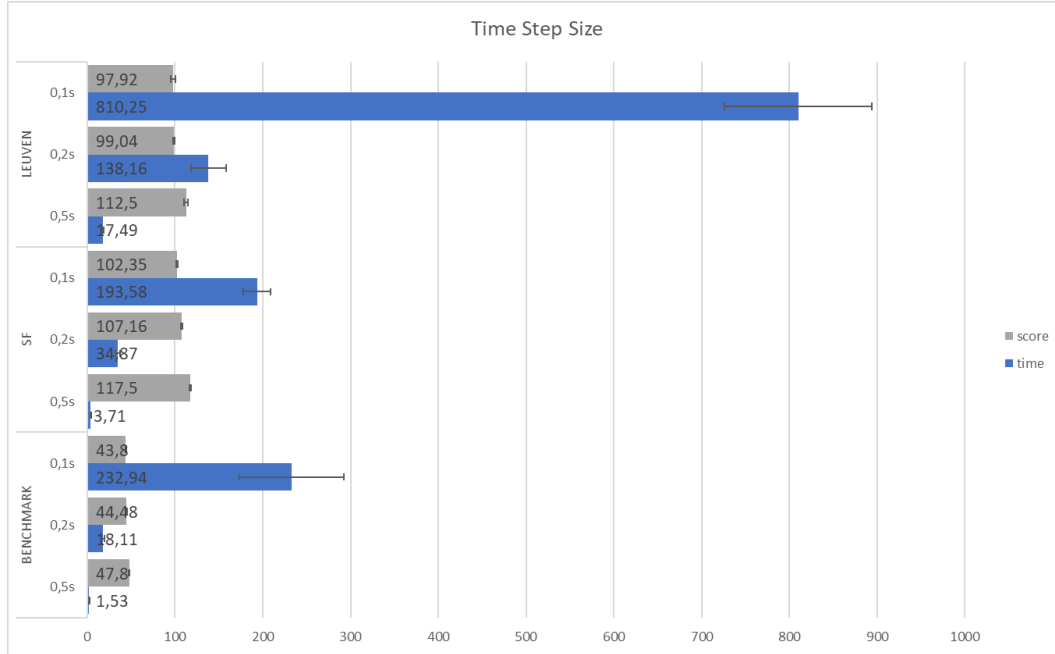


Figure 5.16: time step data

5.7 Time step size

The time step size determines how many time steps are used in each MILP problem. The discretized time steps are samples at regular intervals of the continuous trajectory that the UAV would actually travel in the real world. As a result, the trajectory defined by those time steps is a piece-wise linear approximation of this smooth, real world trajectory.

As the size of each step goes to zero, the approximation becomes more accurate. This also means that the trajectory should become faster, since the UAV can be controlled more precisely through time. This allows for more aggressive maneuvers. However, adding more time steps increases the amount of integer variables and constraints. This comes at a performance cost.

In this experiment, three different time step sizes are tested. The 0.2s default value, as well as 0.1s and 0.5s are tested.

5.7.1 Interpretation

The time step size has a dramatic impact on performance. Changing the time step size from 0.2s to 0.1s or 0.5s changes the solve time by a factor of 5 to 10 or even more for the Up/Down scenario. This experiment really shows the exponential complexity of MILP. Making the time steps smaller makes the algorithm much slower.

As expected, decreasing the time step size also improves the score of the trajectory. The largest gain is the step from 0.5s to 0.2s, although there still is some improvement when going to 0.1s.

5. EXPERIMENTS AND RESULTS

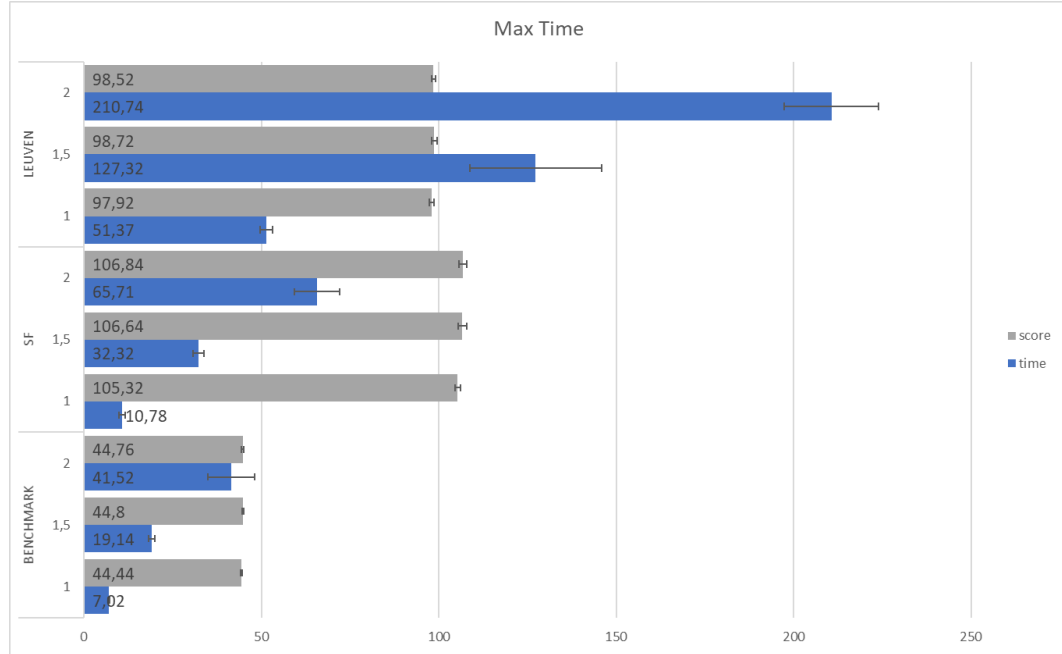


Figure 5.17: maxtime data

5.8 Max Time

For each sub-problem, the amount of time steps to model needs to be determined in advance. The algorithm calculates an estimated upper bound for the time (and thus the amount of time steps). In the ideal case, this upper bound is equal to the time needed for the optimal trajectory. However, if the upper bound is too low, no solution can be found.

This experiment looks at the importance of a low upper bound on the time needed. By default, the estimated upper bound is multiplier by 1.5 to ensure enough time steps are available. A multiplier of 1 is also tested, along with a multiplier of 2.

5.8.1 Interpretation

The time needed to solve the scenarios is heavily influenced by maximum time given. For these scenarios, the default multiplier of 1.5 seems unnecessary and could be lowered to 1 without issues. Increasing the multiplier to 2 nearly doubles the solve time across the board.

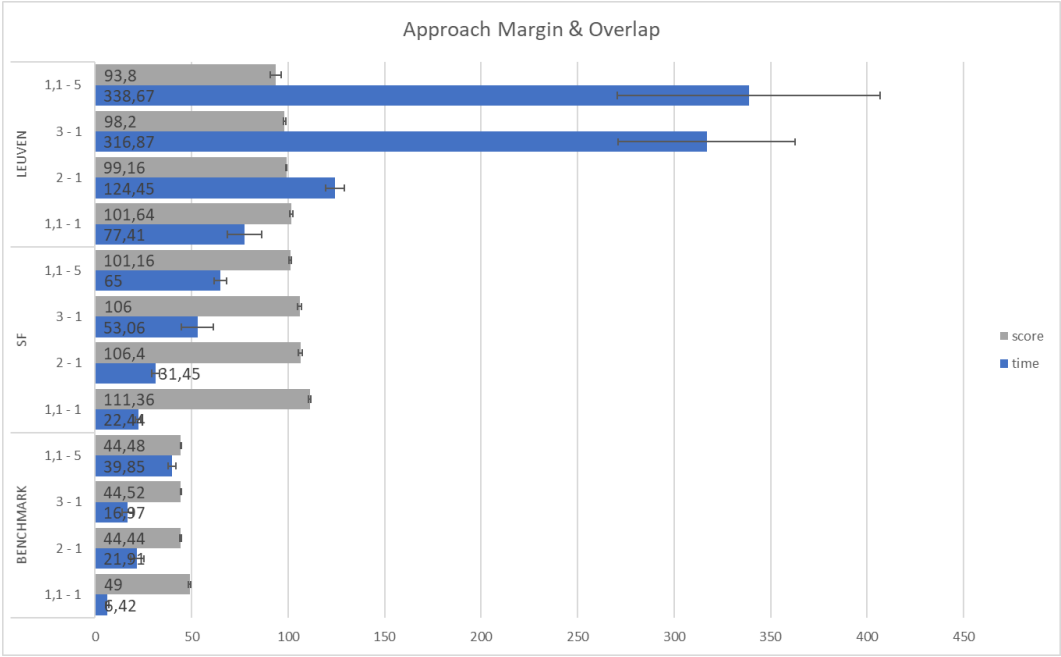


Figure 5.18: approach data

5.9 Approach Margin

TODO

5.9.1 Interpretation

TODO

5.10 Genetic Algorithm Parameters

TODO

Discussion

The goal of this thesis is build a scalable approach for MILP trajectory planning. The target vehicles are multirotor UAVs, so the results in the previous section need to be analyzed in that context.

The first step is analyzing whether or not the approach is actually scalable enough when planning the trajectory for this kind of vehicle through complex environments. Afterwards, the other experiments demonstrate the importance of some of the parameters used in the algorithm. The results provide insight in the limitations of the current approach, and how it may be improved in the future.

6.1 Research question result

The general performance results show that the algorithm is capable of planning a long trajectory through complex environments. Even for the smallest scenarios, the solver struggles to find a trajectory without preprocessing. With my algorithm, the UAV can successfully navigate an entire city.

The convexity test demonstrates that convexity of the search space is indeed a large factor. This supports the assumption that my entire algorithm is built upon: Maintaining convexity as much as possible is required to make the algorithm scale. The stability test shows that, for the most part, my segmentation approach preserves stability. There still are some issues around the transitions between segments, but they can be eliminated by slightly overlapping the segments. This overlap comes at a performance cost, but it also improves the quality of the trajectory. Overall I am not entirely satisfied with the stability of my current implementation, however I do believe the small issues around segment transitions can be resolved.

The results show a large improvement in scalability in certain realistic scenarios, but the choice of those scenarios has drastically impacted the algorithm I have developed.

During development, I have always used realistic approximations of the capabilities of multirotor UAVs. Those can reach high accelerations but have relatively low maximum velocities compared to what fixed-wing aircraft can achieve. This makes those vehicles very agile, which is one of the contributing factors to their recent

popularity.

The assumption of this agility means that my algorithm cannot be applied to UAVs which do not have that property. One of the properties my algorithm uses often is the maximum acceleration distance, which is the distance in which the UAV can always come to a complete stop. This works fine with multirotor UAVs, but is a meaningless concept when dealing with fixed-wing UAVs which cannot stop at all during flight.

However, those kinds of low-agility UAVs are unlikely to be deployed at low altitudes in dense city centers exactly because they lack agility. Even with perfect planning, cities are very unpredictable places. An multirotor UAV is much more likely to be able to safely react to an unexpected obstacle than a fixed-wing UAV.

While I picked out fixed-wing UAVs as an example, the same arguments hold for any kind of UAV that either cannot hover or has low agility. Some UAVs may be able to hover, but are not very agile due to a high maximum velocity and low acceleration. In this case, the agility can be improved by reducing the maximum velocity.

The density of obstacles is also an extremely important factor. The Leuven scenario is significantly harder than the San Francisco scenario because the obstacles are smaller and closer together. Not only are the obstacles closer together, but they are also polygons and can have many more edges per obstacle. For scenarios where the obstacles are significantly denser or complex than in the Leuven scenario, the approach may not improve the performance enough.

On the other hand, the Leuven map is much more detailed than is required for navigation. Many obstacles could be merged together without a significant on possible trajectories. The obstacles could also be simplified, reducing the amount of edges per obstacle. Given that the Leuven map is unprocessed except for calculating the convex hull of each obstacle, the algorithm should be able to handle most real world maps when properly prepared.

Given these considerations, I conclude that my approach meets the basic requirements. The assumptions behind the design of the algorithm seem to be valid based on experiments.

6.2 Factors

While the chosen parameter values allow the algorithm to scale well, different values may be chosen to find a different balance between performance and solution quality. The corner cutting prevention makes the trajectory slightly slower, but that is to be expected since cutting a corner is faster than going around. The performance does take a hit, but the extent is minimal. The corner cutting prevention constraints seem certainly worth being enabled.

The 2-norm approximation has a slightly larger effect on performance. However, there does not seem to be an impact on the trajectory speed. This value could be reduced for a small performance gain.

The time step size and maximum time both have a dramatic impact on the performance. The time step size should be no smaller than necessary, and the maximum time should be as small as possible. They are by far the most important performance factors. As a result, further improvements on performance should focus on these factors. A way to improve performance may be solving each segment twice: Once with a high time step size and a conservative maximum time, and another time with a smaller time step size and a very tight maximum time. The first run quickly and provides a tight upper limit on the amount of time needed for the segment. The second run would also run significantly faster, since the amount of time steps modeled is much closer to what is actually needed. Due to a lack of time, I was unable to implement this.

The approach margin data is probably the strangest. Going from a low to medium approach margin increases the solve time and improves the trajectory, as expected. However, increasing the approach margin again actually decreases the solve time again, as well as reducing the quality of the trajectory. This is unexpected since a approach margin should lead to larger segments which take longer to solve. The larger segments should also improve the quality of the solution because corners can be taken more efficiently, yet the the opposite happens in the data. TODO: find answer?

6.3 Critical Review

Degree of Non-convexity

TODO: intro

7.1 Scenarios

Typically, the amount of integer variables is used as a metric for the difficulty of a MILP problem. The amount of integer variables determines the worst case time needed to solve the MILP problem. An integer variable is needed for every edge, for every obstacle, for every time step. Increasing the amount of time steps and obstacles also increases the time needed to solve.

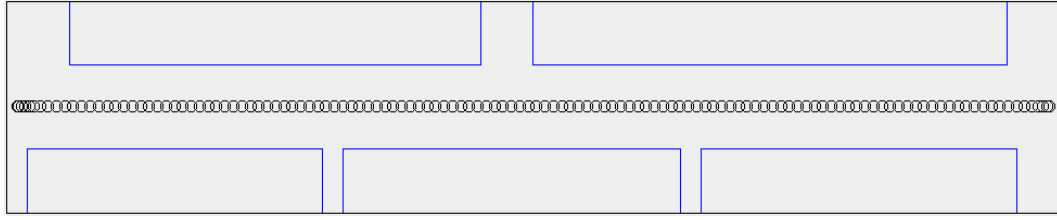
However, the amount of integer variables does not seem to be the only factor that determines the solve time. Figure 7.1 shows three different scenarios, each with the same amount of obstacles. The time step size is $0.2s$, and in each scenario there were 30 seconds worth of time steps. The scenarios are built such that the time needed for the UAV to reach the goal position is roughly the same (between 26 and 27 seconds). As a result, each scenario has the same amount of integer variables. With 4 edges for all 5 obstacles and 150 time steps, they each have 3000 integer variables to model the obstacles alone.

In the Horizontal scenario, the obstacles are not in the way of the UAV. The UAV can move in a straight line from the start position to its goal. In the Diagonal scenario, two of the obstacles are slightly in the way. The UAV is forced to make slight turns near the start and end of the trajectory. However, most of the trajectory is still straight. In the Up/Down scenario, the vehicle has to slalom around every obstacle.

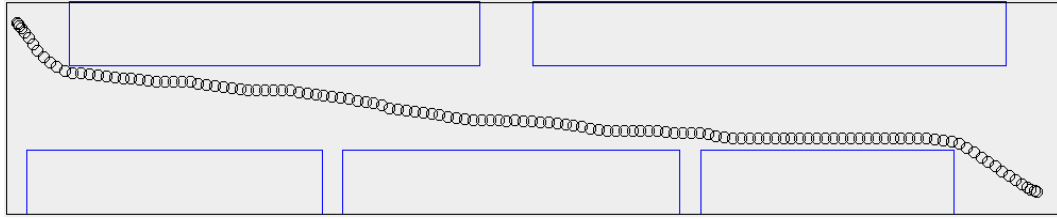
7.2 Results

Each scenario was solved five times. Figure 7.2 shows the time needed to solve the models, as well as the score. The score is also expressed in seconds, and is the time needed for the UAV to reach the goal position when following the generated trajectory.

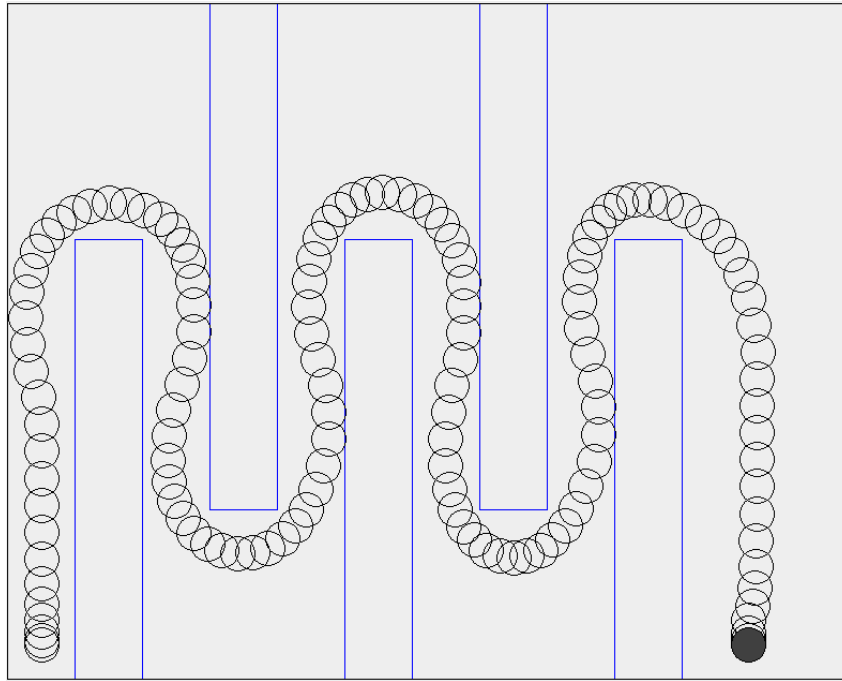
The time needed to solve these scenarios varies dramatically. The Horizontal scenario



(a) The horizontal scenario.



(b) The diagonal scenario.



(c) The Up/Down Scenario.

Figure 7.1: Three different testing scenarios, each with the same amount of obstacles. In each scenario, the UAV needs nearly the same amount of time steps to reach its goal. The only difference is the layout of the obstacles.

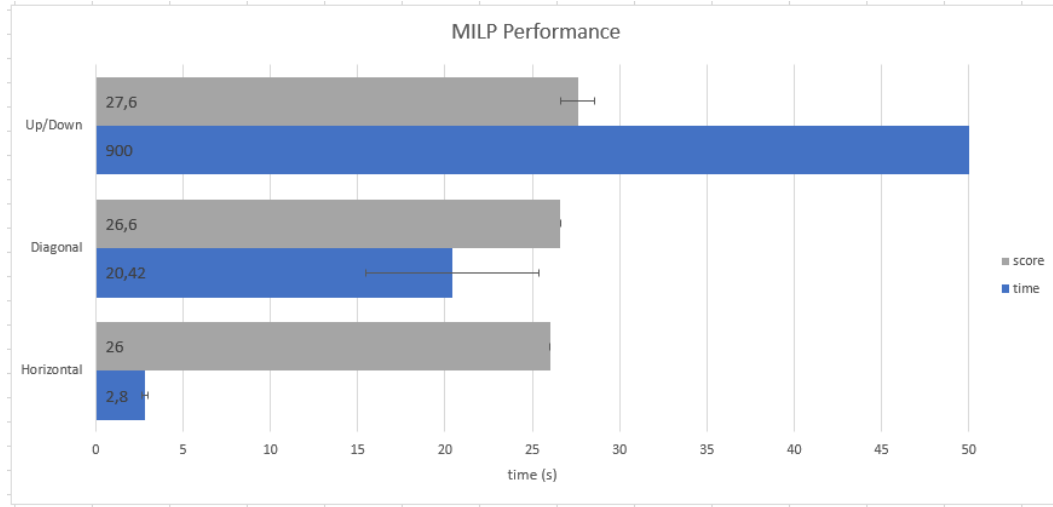


Figure 7.2: Performance of the MILP problem.

is solved consistently in just under 3 seconds. The Diagonal scenario comes in at around 20 seconds, although the 95% confidence interval is $\pm 4.9s$. The Up/Down scenario was limited to 900s of execution time. In this time, the solver could not find the optimal trajectory, which is why the score has a confidence interval.

7.3 Discussion

Intuitively, it is not surprising that the Up/Down scenario is harder to solve than the other two. A human pilot would also have more difficulties navigating the Up/Down scenario compared to the others. However, this cannot be determined by looking at the amount of integer variables or constraints alone.

Problems where the trajectory requires maneuvers seem to be harder to solve. The maneuvers are necessary because there are obstacles blocking a straight approach to the goal position. This observation led me to believe that the integer variables themselves do not cause the poor performance, but the real issue is what they model: a non-convex search space.

The amount of integer variables determines the worst-case performance because it determines the degree to which the search space can be non-convex. An informal definition of this degree of non-convexity would be the minimum amount of (possibly overlapping) convex shapes needed to reconstruct the original shape. With a single boolean variable, you need at most 2 convex shapes. With n boolean variables, at most 2^n convex shapes are needed. TODO: cite.

The degree of convexity of the open space for the Up/Down scenario is 11 as shown in Figure 7.3b. For the Horizontal and Diagonal scenarios, this is 8 as shown in Figure 7.3a. There is a difference, but this still does not seem like a good explanation. The Horizontal and Diagonal scenarios have the same degree of convexity, even though there's almost an order of magnitude difference in the solve times.

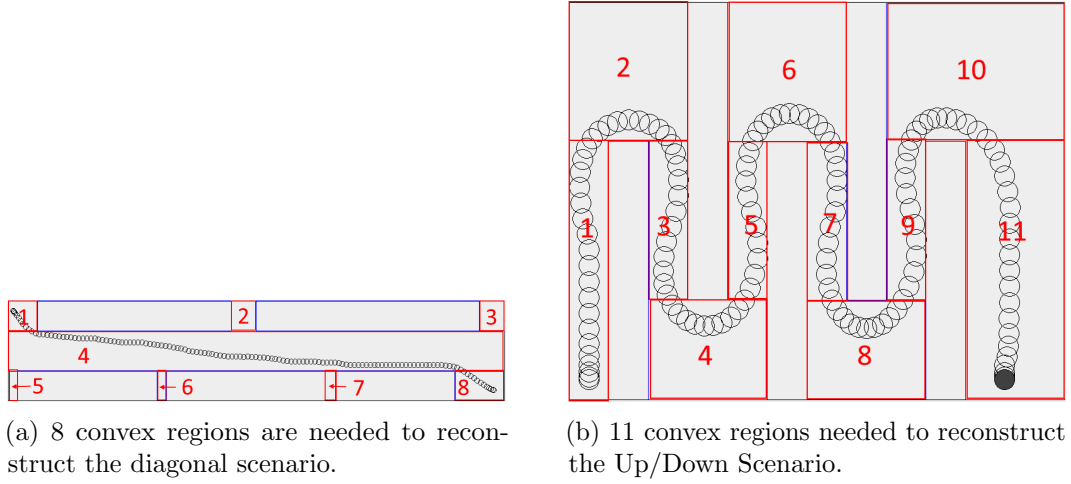


Figure 7.3

Even though the global degree of convexity is the same for the Horizontal and Diagonal scenarios, this is not the case for the neighborhood around the trajectory. In the Horizontal scenario, the trajectory only goes through a single convex region. In the Diagonal scenario, the trajectory goes through 3 convex regions. For the Up/Down scenario, the trajectory goes through all 11 regions. I present the following hypothesis:

Hypthesis 1 *The degree of non-convexity around the optimal trajectory is a better indicator of the time needed to solve a MILP trajectory planning problem than the amount of integer variables.*

Conclusions

Path planning using MIP was previously not computationally possible in large and complex environments. The approach presented in this paper shows that these limitations can effectively be circumvented by dividing the path into smaller segments using several steps of preprocessing. The specific algorithms used in each step to generate the segments can be swapped out easily with variations. Because the final path is generated by a solver, the constraints on the path can also be easily changed to account for different use cases. The experimental results show that the algorithm works well in realistic, city-scale scenarios, even when obstacles are distributed irregularly and dense.

8.1 Future work

The obvious next step is extending this approach to 3D. The extra degree of freedom will likely come at a significant performance penalty, so this was not attempted during the thesis. One of the likely difficulties with the preprocessing as presented is that it treats all dimensions the same. This is fine for the horizontal dimensions, but due to gravity, movements the vertical dimension have different characteristics. The maximum acceleration of the UAV can no longer be assumed to be the same in all directions.

A possible mitigation to the increasing complexity of obstacles may be using a "2.5D" representation. A 2.5D obstacle is a 2D obstacle which also has a height value. This would only need one additional integer variable per obstacle to model. In a city scenario, this may be an acceptable approximation.

Another extension I would try is using moving to Mixed Integer Quadratic programming. Linear approximations to limit the length of vectors works, but it also introduces artifacts into the path. Increasing the amount of constraints that model the norm helps minimize the impact, but comes at a performance cost. Stating those constraints directly as a quadratic function would reduce the amount of constraints needed per time step. Even though the performance cost of a more accurate linear approximation is limited, this could still improve performance while increasing the accuracy of the model. Especially when the problem is also extended to 3D, since this would require the linear approximation of a sphere instead of a circle.

8.2 actual contribution

8.3 goals reached?

8.4 challenges

Bibliography

- [1] John Saunders Bellingham. *Coordination and control of uav fleets using mixed-integer linear programming*. PhD thesis, Massachusetts Institute of Technology, 2002.
- [2] Atif Chaudhry, Kathy Misovec, and Raffaello D’Andrea. Low observability path planning for an unmanned air vehicle using mixed integer linear programming. In *Decision and Control, 2004. CDC. 43rd IEEE Conference on*, volume 4, pages 3823–3829. IEEE, 2004.
- [3] Ian D Cowling, Oleg A Yakimenko, James F Whidborne, and Alastair K Cooke. A prototype of an autonomous controller for a quadrotor uav. In *Control Conference (ECC), 2007 European*, pages 4001–4008. IEEE, 2007.
- [4] Kieran Forbes Culligan. *Online trajectory planning for uavs using mixed integer linear programming*. PhD thesis, Massachusetts Institute of Technology, 2006.
- [5] Robin Deits and Russ Tedrake. Efficient mixed-integer planning for uavs in cluttered environments. In *Robotics and Automation (ICRA), 2015 IEEE International Conference on*, pages 42–49. IEEE, 2015.
- [6] Michele Fliess, Jean Lévine, Philippe Martin, and Pierre Rouchon. Design of trajectory stabilizing feedback for driftless at systems. *Proceedings of the Third ECC, Rome*, pages 1882–1887, 1995.
- [7] Melvin E Flores. *Real-time trajectory generation for constrained nonlinear dynamical systems using non-uniform rational B-spline basis functions*. PhD thesis, California Institute of Technology, 2007.
- [8] Yongxing Hao, Asad Davari, and Ali Manesh. Differential flatness-based trajectory planning for multiple unmanned aerial vehicles using mixed-integer linear programming. In *American Control Conference, 2005. Proceedings of the 2005*, pages 104–109. IEEE, 2005.
- [9] Leslie Lamport. A simple approach to specifying concurrent systems. *Communications of the ACM*, 32(1):32–45, 1989.

- [10] Daniel Mellinger and Vijay Kumar. Minimum snap trajectory generation and control for quadrotors. In *Robotics and Automation (ICRA), 2011 IEEE International Conference on*, pages 2520–2525. IEEE, 2011.
- [11] G Mitra, C Lucas, S Moody, and E Hadjiconstantinou. Tools for reformulating logical forms into zero-one mixed integer programs. *European Journal of Operational Research*, 72(2):262–276, 1994.
- [12] Tom Schouwenaars, Bart De Moor, Eric Feron, and Jonathan How. Mixed integer programming for multi-vehicle path planning. In *Control Conference (ECC), 2001 European*, pages 2603–2608. IEEE, 2001.

Fiche masterproef

Student: Jorik De Waen

Titel: Scalable Multirotor UAV Trajectory Planning using Mixed-Integer Linear Programming

Nederlandse titel: Schaalbare Traject Planning voor Onbemande Multirotor Luchtvaartuigen met Gemengd Geheeltallig Lineair Programmeren

UDC: 004.8

Keywords: TODO:keywords

Titel van het artikel: Scalable Multirotor UAV Trajectory Planning using Mixed-Integer Linear Programming

Korte inhoud:

TODO

Thesis voorgedragen tot het behalen van de graad van Master of Science in de ingenieurswetenschappen: computerwetenschappen, hoofdoptie Artificiële intelligentie

Promotor: Prof. dr. T. Holvoet

Assessoren: Dr. M. Cruz Torres
Dr. B. Bogaerts

Begeleiders: H. T. Dinh
Dr. M. Cruz Torres